

# Community Concealment from Unsupervised Graph Learning-Based Clustering

Dalyapraz Manatova  
Indiana University

Pablo Moriano  
Oak Ridge National Laboratory

L. Jean Camp  
UNC Charlotte

## Abstract

Graph neural networks (GNNs) are designed to use attributed graphs to learn representations. Such representations are highly beneficial in the unsupervised learning of clusters and community detection. Nonetheless, such inference may reveal sensitive groups, crucial clustered systems, or collective behaviors, thereby raising concerns regarding group-level privacy. Unauthorized community attribution in social and critical infrastructure networks, for example, can expose coordinated asset groups, operational hierarchies, and system dependencies that could be used for surveillance or intelligence gathering. We study a defensive setting in which a network (or defender) seeks to conceal a community of interest while making limited and utility-preserving changes in the network. Our analysis indicates that community concealment is contingent upon two quantifiable factors: the connectivity at the community boundary and the feature similarity between the protected community and its adjacent ones. Informed by these findings, we present a perturbation strategy that rewrites a set of structurally important edges and modifies node features to reduce the distinctiveness leveraged by GNN message passing. The proposed method consistently surpasses DICE in both synthetic benchmarks and real network graphs, including Facebook, Wikipedia, and Bitcoin Transactions, when subjected to identical perturbation budgets. Overall, it achieves median relative concealment improvements of approximately 20–45% on synthetic and real networks. These findings illustrate an effective safeguard against GNN-based community learning, simultaneously emphasizing

ing and addressing sensitive groups' privacy concerns intrinsic to graph learning processes.

## 1 Introduction

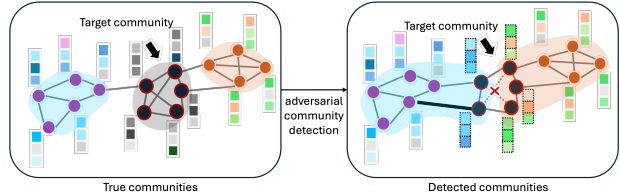


Figure 1: Adversarial community detection scenario. Left: the original network operated by a defender, containing several communities, including one target community that must remain concealed. Right: the output of a GNN used by an adversary to infer community structure. The defender's goal is to modify the graph slightly so that the GNN run by the adversary fails to correctly recover the target community.

Community detection plays a central role in network science and has been widely applied to identify groups of nodes with dense internal connections and shared functions [14, 18, 38]. In social networks, it helps uncover patterns of coordination and collective behavior [41], whereas in critical infrastructure systems, it reveals clusters of assets whose interdependence affects operational resilience [35]. Recent progress in graph neural networks (GNNs) has significantly advanced community detection by integrating structural and feature information [42, 55, 19]. However, this same capability introduces new privacy

risks: GNN-based community detection enables the inference of latent group structure, potentially exposing sensitive collective relationships, operational hierarchies, or dependencies that were previously difficult to infer. This exposure constitutes a form of group-level privacy leakage, such as membership inference or property inference, that cannot be attributed to any single node alone but can be deduced only at the group level, not at the individual level.

Adversaries can leverage GNN-based community detection to extract insights from both network topology and node attributes, uncovering clusters that provide extensive information regarding the networks. Figure 1 illustrates this setting: a defender operates a network that contains one or more communities of interest, while an adversary applies a GNN to infer them. To counter this privacy risk, the defender seeks to modify the graph just enough to ensure that the GNN run by the adversary fails to correctly recover the targeted community [7, 52].

**Problem Formulation.** Community hiding differs from classical community deception [12] because the adversary now employs GNN rather than a modularity-based algorithm. In this setting, the defender aims to reduce the ability of the GNN to correctly identify a targeted community by introducing small, controlled perturbations to the network. These perturbations must preserve key graph properties, such as overall network community structure, since the modified graph must remain functional for legitimate analytics and operations.

The DICE baseline [58] provides a simple heuristic for hiding communities by removing internal links and adding external ones, but its design assumes purely structural detection. GNN-based methods exploit both structure and attributes through message passing, making the defense substantially more complex [19, 55]. This leads to two fundamental questions: *Can a group of nodes (a community) be intentionally hidden from graph-learning-based unsupervised clustering?*

And if so, *what characteristics govern the privacy of a community under a GNN-based community detection algorithm?* A naive extension of DICE often fails to mislead such models, since feature homophily and multi-hop aggregation can still reveal latent commu-

nity boundaries.

These observations define the central challenge: *how to protect group-level privacy by concealing a targeted community from GNN-based inference under a certain perturbation budget.*

Our analysis begins with the observation that the success of community hiding depends on measurable structural and feature-based properties of the network. Through controlled experiments on graphs, we find that the ability to conceal a community from a GNN is strongly influenced by two factors: the ratio of external to internal connections, and the similarity of node features between the targeted community and its neighboring groups. Communities that are weakly connected to the rest of the network or whose features differ sharply from their surroundings tend to be easily rediscovered after perturbation, while those with moderate boundary connectivity and overlapping features are more likely to remain hidden. These findings reveal that community hidability is not uniform but governed by predictable structural and semantic characteristics. Guided by this insight, we design *FCom-DICE* (*Feature-Community-guided DICE*), a defense strategy that extends the structural rewiring of DICE [58] with feature-aware perturbations. The method rewrites a small number of influential edges and minimally adjusts node features to disrupt the message-passing process that GNNs rely on for community inference [19]. Figure 1 (right) conceptually illustrates this intuition: modifications at community boundaries can substantially alter the representation learned by a GNN, causing the targeted community to be incorrectly recovered or merged with others.

**Technical Contributions.** We evaluate the proposed defense through a series of experiments on both synthetic networks and real social and information networks, including Facebook, Wikipedia and Bitcoin transactions. The synthetic datasets allow controlled variation of community separability, feature similarity, and perturbation budgets, while the real graphs provide realistic structural and attribute distributions. Across all settings, FCom-DICE consistently achieves higher concealment effectiveness than DICE [58] under the same perturbation constraints. The median relative improvement ranges from approximately 20% to 45% across synthetic and real

datasets, demonstrating that feature-guided perturbations substantially enhance a defender’s ability to obscure targeted communities. These improvements are obtained while preserving the overall network community structure.

Together, these results confirm that incorporating feature information into the perturbation process offers a principled and practical advantage for defending against GNN-based community detection [19, 55].

In summary, this work makes the following contributions. First, we formulate the problem of defensive community hiding under GNN-based community detection, where a defender seeks to conceal a targeted community through small, utility-preserving perturbations. Second, through controlled experiments, we identify two measurable factors that govern community hidability: the ratio of external to internal connectivity and the similarity of node features between neighboring communities. Third, we introduce FCom-DICE, a defense strategy that extends DICE by incorporating feature-aware edge rewiring and budgeted feature adjustment to disrupt GNN message passing. Fourth, we conduct a comprehensive evaluation on synthetic networks and real ones, demonstrating that FCom-DICE consistently outperforms DICE, the difference is especially apparent when communities are loosely connected to the rest of the network. Finally, we discuss the implications of these findings for protecting high-value communities in operational and critical infrastructure networks.

## 2 Threat Model and Privacy Setting

We consider a privacy inference setting in which a network operator releases or analyzes an attributed graph for legitimate purposes while seeking to protect a sensitive group from unauthorized inference. Nodes represent entities (e.g., users, assets, or accounts), edges encode relationships or interactions, and node attributes capture metadata or behavioral features.

**Adversary.** The adversary is an analyst with access to the graph structure and node attributes who ap-

plies unsupervised GNN-based community detection to infer latent communities. The adversary’s goal is to recover group membership or organizational structure that is not explicitly disclosed in the data.

**Privacy Risk.** Successful community inference reveals sensitive group-level information, such as coordinated behavior, functional units, or operational dependencies. This constitutes group-level privacy leakage, as the sensitive information emerges only through collective inference rather than individual node attributes.

**Defender and Scope.** The defender controls the graph representation and applies small, utility-preserving perturbations prior to analysis or release. We do not provide formal privacy guarantees; instead, we study practical privacy risks arising from GNN-based community inference, identify characteristics that increase group-level privacy, and propose a method that improves concealment effectiveness over a benchmark approach under the same perturbation budgets.

## 3 Background

We begin with preliminary definitions and background to provide context for the problem investigated in this paper.

### 3.1 Graphs

A graph is defined as  $G = (V, E)$ , where  $V = (v_1, \dots, v_n)$ ,  $|V| = n$  is the set of nodes and  $E \subseteq V \times V$ ,  $|E| = m$  is the set of edges. Each node  $v \in V$  can also have an associated feature vector  $\mathbf{x}_v \in \mathbb{R}^d$ . We denote the collection of all node features by  $\mathbf{X} = \{\mathbf{x}_1, \mathbf{x}_2, \dots, \mathbf{x}_n\}$ , where  $\mathbf{x}_i \in \mathbb{R}^d$  is a  $d$ -dimensional feature vector corresponding to node  $v_i$ . A representation of edges between nodes in a matrix form is defined as an  $n \times n$  adjacency matrix of  $G$ , denoted by  $\mathbf{A}$ , where  $\mathbf{A}_{ij} = 1$  if and only if  $\{v_i, v_j\} \in E$  and otherwise entries of  $\mathbf{A}$  are equal to 0.

## 3.2 Community Detection

A *community* (or cluster), in the graph context, refers to a subgraph  $C_i$  of graph  $G$  where nodes are densely connected inside  $C_i$  and loosely connected with nodes from  $C_j$ , where  $i \neq j$  and  $C_i \cap C_j = \emptyset$  for all  $i, j$  [14]. Here, we assume non-overlapping communities. A community detection algorithm seeks to partition the graph  $G$  into such clusters (i.e., subgraphs)  $\mathcal{C} = \{C_1, \dots, C_k\}$ . A quality of such partitions is often measured by *modularity*, which quantifies the deviation of the intra-cluster edges in the graph  $G$  from the expected number of edges in the random graph [38]. In a random graph, where nodes  $v_i$  and  $v_j$  with degrees  $\hat{k}_i$  and  $\hat{k}_j$  are connected with probability  $\hat{k}_i \hat{k}_j / 2m$ . Then modularity is defined as:

$$Q = \frac{1}{2m} \sum_{i,j} \left( \mathbf{A}_{ij} - \frac{\hat{k}_i \hat{k}_j}{2m} \right) \delta(c_i, c_j) \quad (1)$$

where  $Q$  is the modularity score,  $m$  is the total number of edges in the network,  $\mathbf{A}_{ij}$  is the adjacency matrix entry,  $\hat{k}_i$  and  $\hat{k}_j$  are the degrees of nodes  $v_i$  and  $v_j$ , and  $\delta(c_i, c_j)$  is 1 if nodes  $v_i$  and  $v_j$  are in the same community, 0 otherwise.

There are numerous ways to detect communities in graphs, considering different underlying assumptions, some of the most commonly used methods seek to optimize modularity [3, 39, 54, 11]. Since maximizing modularity is an NP-hard problem [5], a common approach is to relax the discrete optimization into a spectral formulation. Specifically, the modularity function  $Q$  can be rewritten in matrix form [37] as:

$$\mathbf{Q} = \frac{1}{2m} \text{Tr} (\mathbf{C}^\top \mathbf{B} \mathbf{C}), \quad (2)$$

where:

- $\mathbf{C} \in \{0,1\}^{n \times k}$  is a community membership matrix, where  $C_{ij} = 1$  if node  $v_i$  belongs to community  $C_j$  and 0 otherwise,
- $\mathbf{B} = \mathbf{A} - \frac{\mathbf{k}\mathbf{k}^\top}{2m} \in \mathbb{R}^{n \times n}$  is the modularity matrix, with  $\mathbf{k}$  as a degree vector,
- $\text{Tr}(\cdot)$  is the trace matrix operator.

## 3.3 Community Hiding

Community hiding refers to the process of modifying a graph so that a specific group of nodes (i.e., community) is no longer detected as a single group by a community detection algorithm. One of the popular methods (Disconnect Internally Connect Externally (DICE) [58]), which is considered to be a benchmark, randomly rewrites intra-community edges to outside nodes under a fixed perturbation budget  $b$ .  $b$  defines the total number of edge modifications (i.e., deletions and additions) applied to the graph.

To measure the degree to which a group of nodes is successful at hiding, there are several metrics [13, 7], but the commonly used ones are derived by Waniek et al. [58].

Assuming there is a community  $C^*$ , or a target community, aimed to be concealed within other communities in  $G$ , then  $M_1$  is defined by:

$$M_1(C^*, \mathcal{C}) = \frac{|\{C_i \in \mathcal{C} : C_i \cap C^* \neq \emptyset\}| - 1}{\max(|\mathcal{C}| - 1, 1) \times \max_{C_i \in \mathcal{C}} (|C_i \cap C^*|)} \quad (3)$$

Thus,  $M_1$  quantifies how well the nodes of  $C^*$  are spread out across the communities in  $G$ .

Similarly,  $M_2$  is defined by:

$$M_2(C^*, \mathcal{C}) = \sum_{C_i : C_i \cap C^* \neq \emptyset} \frac{|C_i \setminus C^*|}{\max(n - |C^*|, 1)} \quad (4)$$

where  $C_i \setminus C^*$  denotes the set of nodes in community  $C_i$  that are not members of  $C^*$ .  $M_2$  quantifies how well nodes of  $C^*$  are “hidden in the crowd” with other nodes  $V \setminus C^*$ . Both metrics,  $M_1$  and  $M_2$ , have values in the range  $[0, 1]$  where higher values indicate that the target community  $C^*$  is more effectively hidden, i.e., concealed from a community detection algorithm.

## 3.4 GNNs

There is a growing body of work focused on improving community detection by incorporating additional information on nodes’ attributes and their connections [2, 42, 55]. These enhanced methods leverage both network structure and node features to produce

more refined and informed community assignments. GNNs have emerged as a powerful approach in this context, as they integrate node attributes with graph topology, performing nonlinear feature aggregation to learn expressive node embeddings.

Let  $\mathbf{H}^{(l)} \in \mathbb{R}^{n \times d_l}$  denote the node-embedding, where the  $i$ -th row  $\mathbf{H}_{i:}^{(l)}$  is the  $d_l$ -dimensional representation of the node  $v_i$  at the layer  $l$ , and  $\mathbf{H}^{(0)} = \mathbf{X}$ , the original node feature matrix. A generic GNN layer can be written in matrix form as:

$$\mathbf{H}^{(l+1)} = \phi^{(l)} \left( \mathbf{H}^{(l)}, \text{AGG}^{(l)}(\mathbf{A}, \mathbf{H}^{(l)}) \right), \quad (5)$$

where  $\text{AGG}^{(l)}(\mathbf{A}, \mathbf{H}^{(l)}) \in \mathbb{R}^{n \times d_l}$  is a neighborhood aggregation operator that mixes each node's representation with those of its graph neighbors based on  $\mathbf{A}$ , and  $\phi^{(l)}(\cdot)$  is a learnable update function applied row-wise to produce the next-layer representations  $\mathbf{H}^{(l+1)}$ . After  $L$  layers of updates, the final matrix  $\mathbf{H}^{(L)}$  serves as the learned node embedding space. Different GNN architectures (e.g., GCN [24], GraphSAGE [20], GAT [57]) mainly differ in the design of  $\text{AGG}^{(l)}$  and  $\phi^{(l)}$ .

One widely used instantiation of this framework is the GCN. In GCN, aggregation is implemented via a normalized adjacency matrix defined by:

$$\tilde{\mathbf{A}} = \hat{\mathbf{D}}^{-\frac{1}{2}} (\mathbf{A} + \mathbf{I}_n) \hat{\mathbf{D}}^{-\frac{1}{2}}, \quad (6)$$

where  $\mathbf{I}_n$  is the  $n \times n$  identity matrix and  $\hat{\mathbf{D}}$  is the diagonal degree matrix of  $(\mathbf{A} + \mathbf{I}_n)$ , i.e.,  $\hat{\mathbf{D}}_{ii} = \sum_j (\mathbf{A} + \mathbf{I}_n)_{ij}$ .

Using this normalized adjacency matrix, node features are updated through the following transformation:

$$\mathbf{H}^{(l+1)} = \sigma \left( \tilde{\mathbf{A}} \mathbf{H}^{(l)} \mathbf{W}^{(l)} \right), \quad (7)$$

where  $\mathbf{W}^{(l)} \in \mathbb{R}^{d_l \times d_{l+1}}$  is a trainable weight matrix and  $\sigma(\cdot)$  is a nonlinear activation (e.g., ReLU).

Learning in GNNs is driven by a loss function  $\mathcal{L}$  that guides how the weight matrix  $\mathbf{W}^{(l)}$  in each layer is updated during the training. During training, gradients of the loss with respect to the weights are computed via backpropagation and each weight matrix  $\mathbf{W}^{(l)}$  is updated using gradient descent, i.e.,  $\mathbf{W}^{(l)} \leftarrow \mathbf{W}^{(l)} - \alpha \frac{\partial \mathcal{L}}{\partial \mathbf{W}^{(l)}}$ , where  $\alpha$  is the learning rate.

In supervised learning settings, GNNs are typically trained to predict node labels by minimizing a classification loss (e.g., cross-entropy) on a labeled subset of nodes. In unsupervised settings where true labels are not available, GNNs are trained to optimize alternative objectives. For representation learning, this may involve a reconstruction-based loss [23], while in clustering tasks, the objective often targets community quality measures such as modularity [55] or normalized cut [29]. Once the node embeddings are learned, clustering is performed directly on these representations to infer community assignments.

## 4 Methods

### 4.1 LFR Benchmark

We conduct our experiments on synthetically generated networks, where we can precisely control the edge density both within and between communities. To simulate realistic community structures, we use the Lancichinetti–Fortunato–Radicchi (LFR) benchmark generator [28], a widely adopted method that produces graphs with ground-truth community labels. LFR is specifically designed to generate graphs closely resembling properties observed in real-world networks [14, 26, 65].

Each node is assigned a degree drawn from a power-law distribution with exponent  $\alpha$ , constrained by a specified average degree  $\langle \hat{k} \rangle$  and a maximum degree  $\hat{k}_{max}$ . Edges are then assigned such that  $1 - \mu$  of each node's connections lie within its community, and a fraction  $\mu$  connects to nodes outside the community. As  $\mu \rightarrow 0$ , almost all edges are internal (strong, well-separated communities), whereas as  $\mu \rightarrow 1$ , most edges are external (communities become indistinguishable). Around  $\mu \approx 0.5$ , each node has roughly as many external as internal edges, indicating the boundary beyond which communities are no longer defined in the strong sense [28]. Community sizes are also drawn from a power-law distribution, parameterized by the exponent  $\beta$  and  $s_{min}$  as a minimum size and constrained by the following:  $s_{min} > \hat{k}_{min}$  and  $s_{max} > \hat{k}_{max}$ .

In our experiments, we generate networks using the

LFR benchmark model with  $N = 1,000$  and investigate the effect of community hiding with several controlled parameters, such as the mixing parameter  $\mu$  and minimal community sizes  $s_{\min}$ . The full set of parameters used in our experiments is summarized in Table 1.

Table 1: Experimental Configuration Parameters.

Parameter	Value
<i>LFR parameters</i>	
$N$	Number of nodes
$\hat{k}_{\max}$	Maximum degree
$\langle \hat{k} \rangle$	Average degree
$s_{\min}$	Minimum community size
$\alpha$	Degree distribution exponent
$\beta$	Community size distribution exponent
$\mu$	Mixing parameter
$\sigma_c$	Feature centroid separation
<i>DICE parameters</i>	
$\beta_b$	Perturbation budget (% of $ E_{\text{intra}} $ )
$p$	Deletion ratio parameter
<i>Experimental setup</i>	
$r$	Number of realizations

## 4.2 Feature Generation for LFR

To simulate a graph learning scenario for evaluating community hiding methods, we extend the synthetic LFR benchmark by generating node features. Since LFR does not provide node features by default, we generate synthetic features for LFR using a method adapted from Tsitsulin et al. [56] originally proposed for the Stochastic Block Model (SBM) [47].

We assume that LFR produces  $k$  ground-truth communities denoted by  $C_1^{\text{LFR}}, C_2^{\text{LFR}}, \dots, C_k^{\text{LFR}}$ , where each  $C_i^{\text{LFR}} \subseteq V$  and  $C_i^{\text{LFR}} \cap C_j^{\text{LFR}} = \emptyset$  for  $i \neq j$ . To generate aligned node features, we construct  $k$  feature clusters  $\mathcal{C} = \{C_1^f, \dots, C_k^f\}$ , such that each node  $v_j$  has a feature vector  $\mathbf{x}_j \in \mathbb{R}^d$  from a distribution associated with the feature cluster cor-

responding to its community. Formally:

$$v_j \in C_i^{\text{LFR}} \Rightarrow \mathbf{x}_j \sim \mathcal{N}(\mu_i^f, \sigma^2 \mathbf{I}_{d \times d}) \text{ and } \mathbf{x}_j \in C_i^f,$$

where  $\mu_i^f$  is the centroid of the feature cluster  $C_i^f$ . This setup ensures that the node community assignments align with feature clusters, i.e.,  $\mathcal{C} = \{C_1^f, \dots, C_k^f\}$  with  $C_i^{\text{LFR}} \equiv C_i^f$ .

For each feature cluster  $C_i^f$ , we sample a centroid  $\mu_i^f \in \mathbb{R}^d$  from a  $d$ -dimensional multivariate Gaussian distribution with zero mean and standard deviation  $\sigma_c^2$ :

$$\mu_i^f \sim \mathcal{N}(0, \sigma_c^2 \cdot \mathbf{I}_{d \times d}), \quad (8)$$

where  $\sigma_c$  controls the dispersion between the centroids of different clusters. We use  $d = 32$  by default, as it has been used in other studies [56, 19].

Then, for each node  $v_j \in C_i^{\text{LFR}}$ , we generate a feature vector  $\mathbf{x}_j$  by sampling from another  $d$ -dimensional multivariate Gaussian distribution centered at the corresponding centroid  $\mu_i^f$

$$\mathbf{x}_j \sim \mathcal{N}(\mu_i^f, \sigma^2 \cdot \mathbf{I}_{d \times d}), \quad (9)$$

where  $\sigma^2 = 1$  is a fixed intra-cluster variance.

Note that  $\sigma_c$  controls the separation between feature cluster centroids. A higher  $\sigma_c$  means centroids are farther apart, making clusters more separable, while lower values lead to overlapping clusters. When  $\sigma_c$  is much smaller than  $\sigma$  (which we normalize by setting  $\sigma = 1$ ), the feature clusters become highly overlapping, introducing noise that makes cluster boundaries harder to distinguish in feature space, and thus easier to conceal from a community detection algorithm.

This synthetic feature generation process enables us to evaluate how well GNN-based community detection and subsequent community hiding methods perform under varying levels of feature noise.

## 4.3 DICE

A widely used and simple method for community hiding is the DICE (Disconnect Internally, Connect Externally) approach [58]. One of the key advantages of DICE is that it does not require global knowledge of

the entire graph. Instead, it relies on a modularity-inspired heuristic: reduce the internal connectivity of the target community while increasing its external connectivity to the rest of the network.

The algorithm is stochastic and follows a two-step approach: (1) edge deletion inside the community and (2) edge addition to external nodes. Thus, given:

- a target community  $C^* \subseteq G$ ,
- a total perturbation budget  $b \in \mathbb{N}$  representing the number of edge modifications (deletions plus additions), and
- a proportion parameter  $p \in [0, 1]$  that defines the fraction of the budget allocated to edge deletions (with the remaining  $1 - p$  fraction assigned to edge additions),

the algorithm proceeds as in Algorithm 1,

---

**Algorithm 1** DICE

---

**Input:**  $G = (V, E)$ ,  $C^* \subseteq V$ ,  $b \in \mathbb{N}$ ,  $p \in [0, 1]$   
**Output:** Perturbed graph  $G' = (V, E')$   
 $G' \leftarrow G$ ;  $b_{\text{del}} \leftarrow \lfloor b \cdot p \rfloor$ ;  $b_{\text{add}} \leftarrow b - b_{\text{del}}$   
1. *Intra-community edge deletion*  
 $E_{\text{intra}} \leftarrow \{(u, v) \in E \mid u \in C^*, v \in C^*\}$   
Randomly sample  $E_{\text{del}} \subseteq E_{\text{intra}}$  such that  $|E_{\text{del}}| = \min(b_{\text{del}}, |E_{\text{intra}}|)$   
Remove edges  $E_{\text{del}}$  from  $G'$   
2. *External edge addition*  
 $V_{\text{ext}} \leftarrow V \setminus C^*$   
 $\mathcal{E}_{\text{cand}} \leftarrow \{(u, v) \in C^* \times V_{\text{ext}} \mid (u, v) \notin E\}$   
Randomly sample  $E_{\text{add}} \subseteq \mathcal{E}_{\text{cand}}$ , such that  $|E_{\text{add}}| = \min(b_{\text{add}}, |\mathcal{E}_{\text{cand}}|)$   
Add edges  $E_{\text{add}}$  to  $G'$   
 $E' \leftarrow (E \setminus E_{\text{del}}) \cup E_{\text{add}}$   
**return**  $G' = (V, E')$

---

where:

- $b_{\text{del}}, b_{\text{add}} \in \mathbb{N}$  are the number of intra-community edges to delete and external edges to add, respectively,
- $E_{\text{intra}} \subseteq E$  is the set of edges within the target community  $C^*$ ,

- $V_{\text{ext}} = V \setminus C^*$  is the set of nodes outside of the target community,
- $\mathcal{E}_{\text{cand}} = \{(u, v) \in C^* \times V_{\text{ext}} \mid (u, v) \notin E\}$  is the set of all possible cross-community edges that can be added (i.e., edges not yet present in  $G$ ), and
- $E_{\text{del}} \subseteq E_{\text{intra}}$  and  $E_{\text{add}} \subseteq \mathcal{E}_{\text{cand}}$  are randomly sampled sets of edges to delete and add, respectively,
- the final output is a perturbed graph  $G' = (V, E')$  with edge set  $E' = (E \setminus E_{\text{del}}) \cup E_{\text{add}}$ .

#### 4.4 DMoN

We apply Deep Modularity Networks (DMoN) [55], a GCN-based unsupervised clustering method, to detect communities in the perturbed and original graphs. DMoN has attained state-of-the-art outcomes, generating high-quality clusters that exhibit a strong correlation with ground truth labels [55], and the method has demonstrated significant resilience against targeted and adversarial perturbations when compared to other state-of-the-art unsupervised clustering methods such as DiffPool and MinCutPool [19].

DMoN learns soft cluster assignments by optimizing a modularity-based objective in an end-to-end manner. The method follows two main steps: (1) node representation learning via graph convolutions, and (2) soft cluster assignments computed through differentiable pooling. Instead of using standard GCN with self-loops, DMoN replaces the self-loop mechanism with a learnable skip connection to better preserve raw node features. The forward pass in the encoder is defined as:

$$\mathbf{H}^{(l+1)} = \text{SeLU} \left( \hat{\mathbf{A}} \mathbf{H}^{(l)} \mathbf{W} + \mathbf{X} \mathbf{W}_{\text{skip}} \right), \quad (10)$$

where  $\mathbf{W}_{\text{skip}} \in \mathbb{R}^{d \times d}$  is a learnable skip connection matrix applied to the original features  $\mathbf{X}$ ,  $\hat{\mathbf{A}} = \mathbf{D}^{-\frac{1}{2}} \mathbf{A} \mathbf{D}^{-\frac{1}{2}}$  is normalized adjacency matrix without self-loops, and SeLU is the Scaled Exponential Linear Unit activation [25].

Given the final layer node representations  $\mathbf{H} \in \mathbb{R}^{n \times d}$  from the modified GCN, the cluster assignment matrix  $\mathbf{C} \in \mathbb{R}^{n \times k}$  is computed as:

$$\mathbf{C} = \text{softmax}(\text{GCN}(\hat{\mathbf{A}}, \mathbf{X})), \quad (11)$$

where  $k$  is the number of clusters, specified at the beginning of the training. Each row of  $\mathbf{C}$  gives the soft assignment of a node to clusters and is normalized to sum to 1.

To learn these soft assignments, DMoN optimizes the spectral modularity (a relaxed form) objective with the collapse regularization to avoid trivial assignment (i.e., all nodes assigned to one cluster). The loss function is defined as follows:

$$\mathcal{L}_{\text{DMoN}}(\mathbf{C}, \mathbf{A}) = \underbrace{-\frac{1}{2m} \text{Tr}(\mathbf{C}^\top \mathbf{B} \mathbf{C})}_{\text{modularity}} + \underbrace{\frac{\sqrt{k}}{n} \left\| \sum_i \mathbf{C}_i^\top \right\|_F}_{\text{regularization}} - 1,$$

where  $\mathbf{B} = \mathbf{A} - \frac{\hat{\mathbf{k}}\hat{\mathbf{k}}^\top}{2m}$  is a modularity matrix with  $\hat{\mathbf{k}} \in \mathbb{R}^n$  as the degree vector and  $\|\cdot\|_F$  is a Frobenius norm. Note that  $\frac{1}{2m} \text{Tr}(\mathbf{C}^\top \mathbf{B} \mathbf{C})$  is a spectral relaxation of modularity (Eq. (2)) with  $\mathbf{C}$  as the soft cluster assignment matrix from Eq. (11). The regularization constrains the optimization and prevents gradient-based methods from converging to trivial solutions [55]. This regularization term is normalized to lie within the range  $[0, \sqrt{k}]$  and is 0 when clusters are perfectly balanced in size, and  $\sqrt{k}$  when all nodes collapse into a single cluster.

Additionally, to avoid gradient descent becoming trapped in local optima of the highly non-convex objective function, the authors apply dropout [48] to GCN representations before the softmax in Eq. (11).

## 4.5 Experimental Setup

We systematically vary the parameters of the graph, features, and attacks to evaluate how community hidability depends on different factors.

We vary the mixing parameter  $\mu$  across six values  $\{0.01, 0.1, 0.2, 0.3, 0.4, 0.5\}$  to control the level of inter-community edge mixing. Additionally, we vary the feature noise parameter  $\sigma_c$  across  $\{0.01, 0.1, 0.5,$

1, 2, 5\}, and experiment with three different minimum community sizes in LFR: 10, 30, and 60, to explore the impact of community size distribution. These minimum community sizes yield 25, 18, and 12 communities, respectively.

We apply DICE with varying perturbation budgets  $\beta_b$ , where each value corresponds to a different fraction of the total number of intra-community edges in the target community  $C^*$ . Specifically, for each experiment realization, we compute  $b = \lfloor \beta_b |E_{\text{intra}}| \rfloor$ , where  $\beta_b \in [0.01, 1]$  is varied in increments of 0.05. This allows us to simulate perturbations ranging from 1% up to 100% of the available intra-community edges.

We also evaluate performance under different values of the deletion ratio parameter  $p \in \{0, 0.25, 0.5, 0.75, 1\}$ , controlling the balance between internal edge removals  $b_{\text{del}}$  and external edge additions  $b_{\text{add}}$ .

In each run, we apply DICE by focusing on each target community individually and record the evaluation metrics  $M_1$  and  $M_2$  for each case. To ensure robustness against stochastic effects, each experiment is repeated 50 times. The entire set of parameters for experiments is listed in Table 1.

## 5 Results

In this section we present results of our experiments. In Section 5.1 we report the results of community hiding with a baseline technique, DICE, investigating various parameters that affect a target community's hidability. In Section 5.2, we discuss the methods we use to analyze features that contribute to the hidability of a community from DMoN, unsupervised GNN-based clustering. Based on the findings from Sections 5.1 and 5.2, we introduce a novel method, FCom-DICE, which enhances DICE to achieve greater concealment from GNN-based clustering. In Section 5.3 we describe the method, and in Section 5.4 we report results in comparison with the baseline.

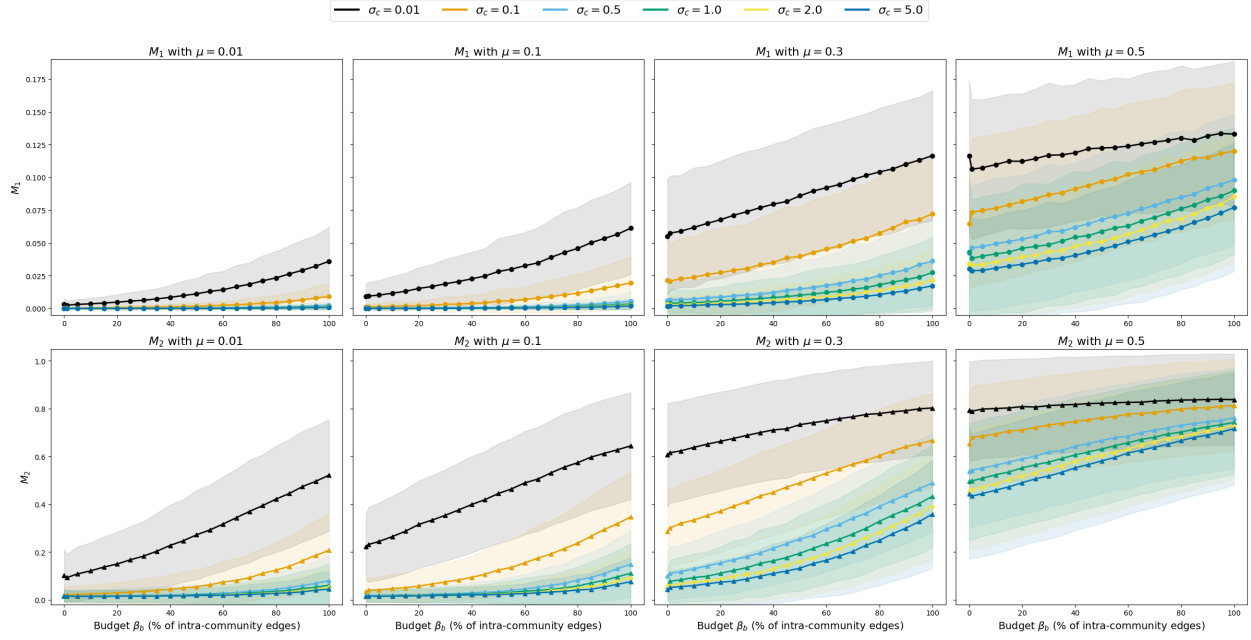


Figure 2: Results of DICE performance with different  $\sigma_c$ ,  $\mu$ , and perturbation budget  $\beta_b$  with  $p = 0.5$  (50% of the  $b$  allocated to deletion vs adding edges) averaged over all realizations. Shaded bands around lines denote  $\pm 1$  s.d. across all runs.

## 5.1 DICE Performance

We start by investigating the performance of DICE with  $p = 0.5$  (the default for DICE), so half of the perturbation budget  $b$  deletes intra-community edges in the target community, and the other half adds new external edges. Figure 2 illustrates two metrics:  $M_1$  (top row) and  $M_2$  (bottom row), as a function of the perturbation budget  $\beta_b$  (x-axis, representing the percentage of intra-community edges perturbed). Columns denote the LFR mixing parameter  $\mu \in \{0.01, 0.1, 0.3, 0.5\}$ . The colored curves represent the feature-space separation parameter  $\sigma_c$  (a smaller  $\sigma_c$  indicates increased overlap/noise), while the bands signify one standard deviation across all realizations of the experiments.

In all plots, an increase in the perturbation budget  $\beta_b$  consistently elevates both metrics  $M_1$  and  $M_2$ , indicating that greater perturbation results in enhanced concealment. An increased mixing pa-

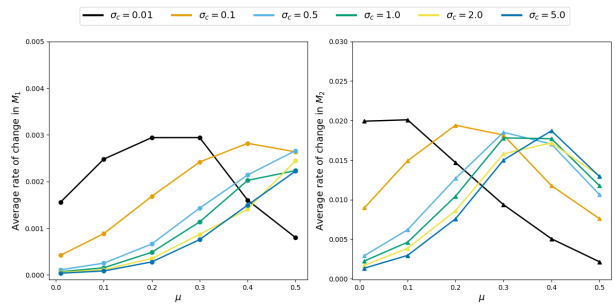


Figure 3: Average rate of change of  $M_1$  and  $M_2$  vs.  $\mu$  for each  $\sigma_c$ .

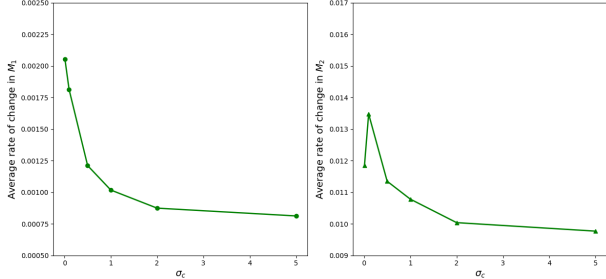


Figure 4: Average rate of change of  $M_1$  and  $M_2$  vs.  $\sigma_c$ , averaged over  $\mu$ .

parameter  $\mu$  elevates the curves for a constant budget  $\beta_b$  and  $\sigma_c$ , indicating that hidability becomes more feasible as the ratio of inter-community edges to intra-community edges increases. Feature noise produces a comparable impact: a smaller  $\sigma_c$  consistently results in higher metric values, as overlapping features obscure boundaries in the embedding space (the arrangement of curves of various colors by  $\sigma_c$  remains stable across the plots in Figure 2). This monotonic effect of  $\sigma_c$  is statistically significant and consistent across all experimental configurations, as confirmed by a one-sided Jonckheere–Terpstra trend test [53, 22, 1] aggregated via Stouffer’s method [50] ( $Z = 361.0, p \ll 10^{-6}$ , one-sided).

Note that  $M_1$ , although theoretically in the same range as  $M_2$  (between 0 and 1) remains small in magnitude in all conditions (at most  $\approx 0.175$  in our experiments), while still increasing gradually with  $\beta_b$ . Note that such a low magnitude of  $M_1$  is typically observed in other studies as well [29]. Separation between  $\sigma_c$  curves is subtle at low  $\mu$ , however, becomes more apparent as  $\mu$  increases.  $M_2$ , on the other hand, spans a much wider range and reacts more strongly to both  $\mu$  and  $\sigma_c$ : for  $\mu \in \{0.01, 0.1\}$  the increase with budget is roughly linear, while for  $\mu \in \{0.3, 0.5\}$  the rise plateaus (approaching  $M_2 \approx 0.8$  at  $\mu = 0.5$  with  $\sigma_c = 0.01$ ).

Figure 3 shows the average finite rate of change of  $M_1$  and  $M_2$  with respect to the perturbation budget  $\beta_b$ , computed using mean finite differences ( $\Delta M / \Delta \beta_b$ ) and plotted as a function of  $\mu$ . For  $M_1$  (left plot), when features are extremely overlapped

( $\sigma_c = 0.01$ , black), the marginal gain peaks early (around  $\mu \approx 0.2 - 0.3$ ) and drops as  $\mu$  increases, indicating diminishing returns once there is enough structural noise. However, as features become more separable ( $\sigma_c \geq 0.5$ ), the slope rises consistently with  $\mu$ , maxing at  $\mu = 0.5$ . Thus, with more separable features, adding structural noise makes each increment of the perturbation budget more effective for  $M_1$ , however, with noisy features, added structural noise quickly inflates the effects, diminishing it after  $\mu = 0.3$ . For  $M_2$  (right plot), the pattern is similar. In Appendix A.1 we show more details on this.

The rate of change with highly noisy features ( $\sigma_c = 0.01$ ) reaches its maximum at low  $\mu$  and subsequently declines as  $\mu$  increases, indicating a diminishing returns thereafter. As  $\sigma_c$  increases, creating distinct separation in feature space, the peak shifts to higher values of  $\mu$ ; for instance, at  $\sigma_c = 5$ , the maximum rate of change occurs at  $\mu = 0.4$ .

We plot the average rate of change vs.  $\sigma_c$  and average over  $\mu$  to isolate the impact of feature noise (Figure 4). From Figure 4, we can see that the average rate of change in  $M_1$  decreases as  $\sigma_c$  grows, as the more separable the features (larger  $\sigma_c$ ), the less impact each unit of budget  $\beta_b$  has. For  $M_2$  the pattern is similar but with a small bump at  $\sigma_c = 0.1$  before the overall decline. This could be explained by Figure 3, where a very small  $\sigma_c = 0.01$  yields a high rate only at a small  $\mu$  and then declines linearly, so its average over  $\mu$  is pulled down.

To further examine the performance of DICE, we vary  $p \in [0, 0.25, 0.5, 0.75, 1]$ , which controls how a perturbation budget  $b$  is allocated between deleting intra-community edges and adding inter-community edges ( $1 - p$ ). In Figure 5, each heatmap illustrates the metric value ( $M_1$  at the top and  $M_2$  at the bottom) averaged over all perturbation budgets  $\beta_b$  for various combinations of  $p$ ,  $\sigma_c$ , or  $\mu$ . For both,  $M_1$  and  $M_2$ , increasing  $p$  generally improves hidability, meaning deleting edges inside a community is more effective than adding. The strongest effect of  $p$  is observed when  $\mu$  is large and  $\sigma_c$  is small, indicating structural and feature noise, respectively. Regardless of how the perturbation budget is divided, high  $\mu$  and low  $\sigma_c$  yield the largest value across all heatmaps. The rightmost heatmaps, which represent the aver-

age over  $p$ , indicate that  $\mu$  and  $\sigma_c$  are the predominant factors influencing the outcome of hidability, as values are the highest.

DICE's overall efficacy increases with the amount of community structure perturbation (budget  $\beta_b$ ), the proportion of that perturbation devoted to intra-community edge deletion ( $p$ ), the network's existing structural noise ( $\mu$ ), and the overlapping of the node features ( $\sigma_c$ ). Concealment is most difficult when communities are structurally well-separated and features are clean, and easiest when both the network's topology and node features blur community boundaries. When features already blur communities (small  $\sigma_c$ ), additional structural mixing yields smaller incremental benefits as  $\mu$  grows. When features are more separable (larger  $\sigma_c$ ) increasing  $\mu$  initially makes DICE's budget more impactful, but once the network is highly mixed, the marginal returns begin to diminish.

## 5.2 Analysis of Community Hidability

**Methods of Analysis** To understand which properties of communities (before any perturbations)

make them less detectable (more hidable) to GNN-based community detection, we rely on feature importance analysis using SHAP [32]. The background on interpretable ML, particularly feature importance analysis is provided in Appendix A.2.

For each community in our experiments, we compute measures that characterize both the internal structure of the community and its relation to the broader network. These include node-level centrality statistics averaged over the community, as well as community-level metrics obtained by treating a community as a single aggregated node, “super-node” [49]. The complete set of measures and their definitions is provided in Table 2.

In addition to structural measures, we compute feature-space separability of the target community  $C^*$  with a per-community distance descriptor  $\overline{d^2}(C^*)$  defined by:

$$\overline{d^2}(C^*) = \frac{1}{|\mathcal{C}| - 1} \sum_{C_i \in \mathcal{C} \setminus \{C^*\}} \|\mu_{C^*} - \mu_{C_i}\|_2^2, \quad (12)$$

where  $\mathcal{C} = \{C_1, \dots, C_k\}$  denotes the set of communities (aligned across LFR and node features, i.e.,

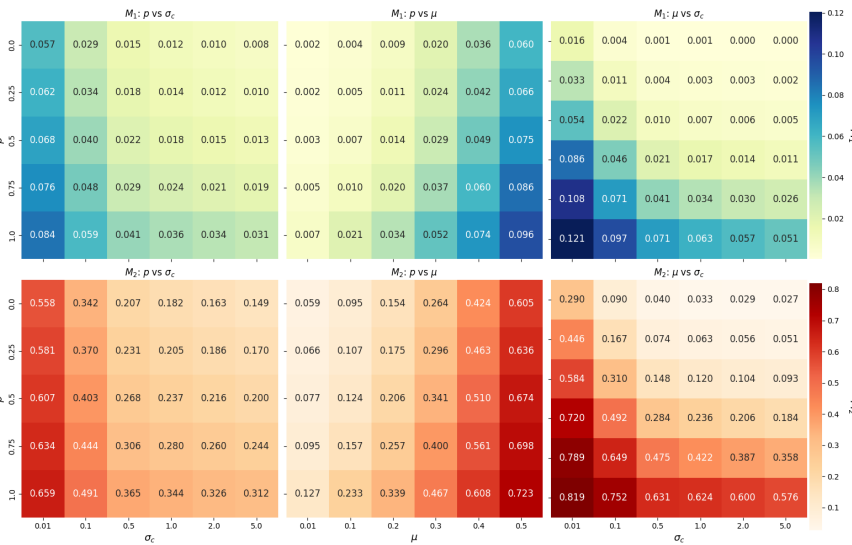


Figure 5: Heatmaps of  $M_1$  and  $M_2$  results of DICE performance with a combination of different  $\sigma_c$ ,  $\mu$ , and  $p$  averaged over all realizations, community labels and all  $\beta_b$ .

Table 2: Measures used for community hidability analysis.

Measure	Notation	Description
Average centroid sq. distance	$\bar{d}^2(C^*)$	Average squared Euclidean distance from the community $C^*$ centroid to all other community centroids based on node features $\mathbf{X}$ .
Community size	$ C^* $	Number of nodes in the community $C^*$
Inter/Intra-edge ratio	$ E_{\text{inter}} / E_{\text{intra}} $	Ratio of external to internal edges of $C^*$
Mean degree centrality	$\bar{k}_u, u \in C^*$	Average degree centrality of nodes in $C^*$
Community degree centrality	$\hat{k}_{C^*}$	Degree of $C^*$ as a super-node, i.e., number of edges leaving $C^*$
Mean betweenness centrality	$\bar{\text{betw}}(u), u \in C^*$	Average betweenness centrality of nodes in $C^*$ (fraction of shortest paths that pass through a node [15])
Community betweenness	$\text{betw}(C^*)$	Betweenness of $C^*$ treated as a super-node (fraction of shortest paths between other communities that pass through $C^*$ )
Mean closeness centrality	$\bar{\text{clos}}(u), u \in C^*$	Average closeness of nodes in $C^*$ (average shortest distance from a node to all other nodes [16])
Community closeness	$\text{clos}(C^*)$	Closeness of $C^*$ as a super-node

Note:  $C^*$  denotes the target community of an experiment.

$C_i^{\text{LFR}} \equiv C_i^f \equiv C_i$ ), and  $\mu_{C_i} = \frac{1}{|C_i|} \sum_{v \in C_i} x_v$  is the centroid (average vector) of community  $C_i$  in a node feature space  $\mathbf{X}$ .

We then apply Random Forest Regression [6] and SHAP analysis to determine which features contribute most to the *hidability* of a community, as measured by  $M_1$  and  $M_2$ . We model  $M_1$  and  $M_2$  independently, with predictors from Table 2, randomly partitioning the data into 80% training and 20% testing. We fit a `RandomForestRegressor` (with default parameters) and report performance as  $R^2$  on the test set. We then compute SHAP values using `TreeExplainer` on the test set and aggregate the absolute SHAP values across the data samples to derive global importance and rank the features accordingly.

**Important Features for Hidability** With Random Forest Regression, we obtain a moderate predictive performance for both metrics ( $R^2 = 0.55$  for  $M_1$  and  $R^2 = 0.69$  for  $M_2$ ). We observe that for both metrics  $|E_{\text{inter}}|/|E_{\text{intra}}|$  (inter/intra-edge ratio) is the most influential predictor, followed by  $\bar{d}^2(C^*)$ , the average centroid distance to other communities in  $\mathbf{X}$ . These two features explain 86% of the total importance for  $M_1$  and 79% for  $M_2$  (see Table 3).

Note that in both metrics ( $M_1$  and  $M_2$ ), higher

Table 3: Normalized global SHAP feature importances for  $M_1$  and  $M_2$ .

Feature	$M_1$ Importance	$M_2$ Importance
$ E_{\text{inter}} / E_{\text{intra}} $	0.487 (0.487)	0.452 (0.452)
$\bar{d}^2(C^*)$	0.373 (0.860)	0.334 (0.787)
$\bar{\text{clos}}(u)$	0.047 (0.907)	0.124 (0.911)
$\bar{\text{clos}}(C^*)$	0.025 (0.932)	0.037 (0.948)
$\bar{k}_u$	0.021 (0.953)	0.015 (0.980)
$ C^* $	0.018 (0.971)	0.018 (0.965)
$\bar{\text{betw}}(u)$	0.017 (0.988)	0.012 (0.992)
$\bar{\text{betw}}(C^*)$	0.010 (0.998)	0.006 (0.998)
$\hat{k}_{C^*}$	0.002 (1.000)	0.002 (1.000)

Note: The importance score in the parentheses is reported as cumulative share.

values of  $|E_{\text{inter}}|/|E_{\text{intra}}|$  (i.e., more external vs. internal edges) tend to increase the predicted value, and lower values of  $\overline{d^2}(C^*)$  (i.e., higher average similarity to other communities in  $\mathbf{X}$  space) also tend to push the predictions upward (see Appendix A.3 for details). Thus, more external edges inside the target community and higher similarity of node features with other communities are important variables for hidability measured by  $M_1$  and  $M_2$ . A complete ranking with normalized (sum-to-1) importances and cumulative shares is presented in Table 3.

### 5.3 Proposed Method: FCom-DICE

**Intuition.** Our experimental analysis of DICE and SHAP analysis indicates that to hide from GNN-based community detection, the structural property of a target community is not the sole characteristic that affects its hidability. The two most significant predictors of hidability are (*i*) the inter/intra-edge ratio and (*ii*) the proximity of the target community to others based on node features. The effectiveness of DICE in hiding a target community is also enhanced when there exists pre-existing structural and node feature-based noise. In other words, concealment improves not only when structural boundaries become indistinct but also when node characteristics of the target community resemble those of other communities. This is consistent with how DMoN (and GNNs broadly) learns node representations and cluster assignments, aggregating node features from neighbors for each node.

This leads to the core intuition behind our method: perturbation should be node feature-aware, along with structural modifications (adding/deleting edges). Therefore, instead of adding edges arbitrarily (as in DICE), we propose that a target community’s nodes should attach to communities that are closest in node feature space so that newly created cross-community edges reinforce the node feature-based signal that pulls embeddings toward the same community in GNN learning. Furthermore, we propose modifications to the node features of the perturbed nodes to enhance their similarity to the newly connected community.

**FCom-DICE: Feature-Community-guided DICE.** Our proposed method, Feature-Community-guided DICE (FCom-DICE), is an adaptation of DICE that adheres to a two-step approach: (1) random edge deletion inside the target community  $C^*$  and (2) edge addition to an external node in the nearest community in feature space, with modification of the node features to the nearest community average. Thus, given:

- a target community  $C^* \subseteq G$ ,
- a total perturbation budget  $b \in \mathbb{N}$  representing the number of edge modifications (deletions plus additions),
- a proportion parameter  $p \in [0, 1]$  that defines the fraction of the budget allocated to edge deletions,
- node features  $\mathbf{X} = \{x_v \in \mathbb{R}^d : v \in V\}$ ,
- the community set  $\mathcal{C} = \{C_1, \dots, C_k\}$  aligned across LFR and features ( $C_i^{\text{LFR}} \equiv C_i^f \equiv C_i$ ), where  $C_i = \{u \in V : c_u = i\}$ ,
- community labels  $\mathbf{c} = (c_1, \dots, c_n)^\top$  with  $c_u \in \{1, \dots, k\}$ , where  $u \in V$ ,
- community feature centroids  $\mu_{C_i} = \frac{1}{|C_i|} \sum_{u \in C_i} x_u$ ,
- and a node-community similarity matrix  $\mathbf{S}_{nc} \in \mathbb{R}^{|V| \times k}$  with entries  $[\mathbf{S}_{nc}]_{ui} = -\|x_u - \mu_{C_i}\|_2^2$ ,

the algorithm proceeds as in Algorithm 2, where:

- $b_{\text{del}}, b_{\text{add}} \in \mathbb{N}$  are the number of intra-community edges to delete and external edges to add, respectively,
- $E_{\text{intra}} \subseteq E$  is the set of edges within the target community  $C^*$ ,
- $G'$  is a perturbed graph with a modified edge set  $E'$
- $V_{\text{ext}} = V \setminus C^*$  is the set of nodes outside of the target community,

- $\mathcal{K}$  is a set of candidate destination communities for a node  $u \in C^*$  with a community label  $c_u$ ,
- $i^\dagger$  is the community label of the *most feature-similar* feasible external community for  $u$ ,
- $\mu_{C_{i^\dagger}}$  is the feature centroid of the community  $C_{i^\dagger}$ ,
- the final output is a perturbed graph  $G' = (V, E')$  with  $\mathbf{X}'$ , which is  $\mathbf{X}$  after all node feature edits.

---

**Algorithm 2** FCom-DICE

---

**Input:**  $G = (V, E)$ ,  $C^* \subseteq V$ ,  $b \in \mathbb{N}$ ,  $p \in [0, 1]$   
**Output:** Perturbed graph  $G' = (V, E')$  with modified node features  $\mathbf{X}'$ .

$G' \leftarrow G$ ;  $b_{\text{del}} \leftarrow \lfloor b \cdot p \rfloor$ ;  $b_{\text{add}} \leftarrow b - b_{\text{del}}$

1. *Intra-community edge deletion*  
 $E_{\text{intra}} \leftarrow \{(u, v) \in E \mid u \in C^*, v \in C^*\}$   
Randomly pick  $E_{\text{del}} \subseteq E_{\text{intra}} \mid |E_{\text{del}}| = \min(b_{\text{del}}, |E_{\text{intra}}|)$   
Remove edges  $E_{\text{del}}$  from  $G'$ :  $E' \leftarrow E \setminus E_{\text{del}}$
2. *External edge addition with node feature modification*  
 $V_{\text{ext}} \leftarrow V \setminus C^*$ ;  $added \leftarrow 0$   
**while**  $added < b_{\text{add}}$  **do**  
  Randomly pick  $u \in C^*$   
   $\mathcal{K} \leftarrow \{i \in \{1, \dots, k\} \setminus \{c_u\} \mid \exists v \in V_{\text{ext}} : c_v = i \wedge (u, v) \notin E'\}$   
  **if**  $\mathcal{K} = \emptyset$  **then**  
    continue  
  **end if**  
   $i^\dagger \leftarrow \arg \max_{i \in \mathcal{K}} [\mathbf{S}_{nc}]_{ui}$   
  Randomly pick  $v \in \{w \in V_{\text{ext}} \mid c_w = i^\dagger, (u, w) \notin E'\}$   
  Add edge  $(u, v)$  to  $G'$ :  $E' \leftarrow (E' \cup (u, v))$   
  Update feature vector for  $u$ :  $x'_u \leftarrow \mu_{C_{i^\dagger}}$   
   $added \leftarrow added + 1$   
**end while**  
**return**  $G' = (V, E')$  with  $\mathbf{X}'$

---

In summary, FCom-DICE differs from DICE in the second step of the algorithm, i.e., edge addition. Rather than attaching to arbitrary external nodes, FCom-DICE selects, for a sampled  $u \in C^*$ , the most feature-similar feasible destination community  $i^\dagger \in \arg \max_{i \neq c_u} [\mathbf{S}_{nc}]_{ui}$ , then chooses a non-neighbor  $v \in C_{i^\dagger}$  and adds the edge  $(u, v)$ . With the edge addition, it modifies features of node  $u$  to the destination community's centroid ( $x'_u \leftarrow \mu_{C_{i^\dagger}}$ ). If no feasible destination exists for the sampled  $u$ , the iteration is skipped to the next sampled node.

The proposed community feature-based edge addition, coupled with feature modification, jointly reduces structural separability (more external than internal ties) and feature separability (greater similarity to a neighboring community).

## 5.4 Evaluation

**Results on Featurized LFR.** In general, FCom-DICE produces higher performance over DICE (baseline) for both metrics,  $M_1$  and  $M_2$ , across different  $\mu$  and  $\sigma_c$ . In Appendix A.4, we present a thorough comparison of the behavior of two methods over the perturbation budget  $\beta_b$ . Here we calculate  $\overline{\Delta M}_1$  and  $\overline{\Delta M}_2$ , the average relative difference (in %) for each  $(\mu, \sigma_c)$  pair, averaged across all perturbation budgets  $\beta_b \in \mathcal{B}$ , all realizations  $r \in \mathcal{R}$ , and all target communities  $C^* \in \mathcal{C}^*$  that are aimed to be concealed, and define it by:

$$\overline{\Delta M}_j(\mu, \sigma_c) = \frac{1}{|\mathcal{B}| |\mathcal{R}| |\mathcal{C}|} \sum_{\beta_b \in \mathcal{B}} \sum_{r \in \mathcal{R}} \sum_{C^* \in \mathcal{C}} \Delta M_j(\beta_b, r, C^*; \mu, \sigma_c), \quad (13)$$

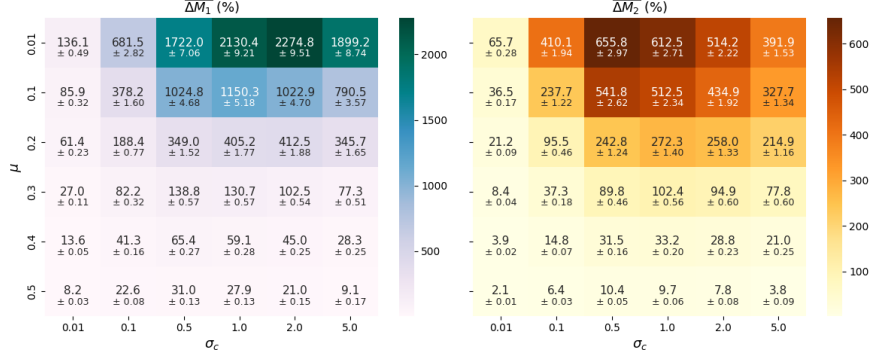


Figure 6: Average relative improvement (%) with  $\pm 1$  s.d.) of FCom-DICE over baseline DICE averaged over all  $\beta_b$  and all realizations. The performance relative difference is shown for various combinations of  $\mu$  and  $\sigma_c$ .

where  $\Delta M_j(\beta_b, r, C^*; \mu, \sigma_c)$  is the percent relative difference between FCom-DICE and DICE when hiding the target community  $C^*$  under budget  $\beta_b$  in realization  $r$ :

$$\Delta M_j(\beta_b, r, C^*; \mu, \sigma_c) = \left( \frac{M_j^{\text{FCom-DICE}} - M_j^{\text{DICE}}}{M_j^{\text{DICE}}} \right) \times 100\%.$$

Here,  $M_j^{\text{FCom-DICE}}$  and  $M_j^{\text{DICE}}$  denote the achieved values of the metric  $M_j \in \{M_1, M_2\}$  for FCom-DICE and DICE, respectively.

The heatmap in Figure 6 illustrates  $\overline{\Delta M_1}(\mu, \sigma_c)$  and  $\overline{\Delta M_2}(\mu, \sigma_c)$ , indicating the degree to which FCom-DICE improves upon the baseline DICE. The improvement is largest when  $\mu$  is small, i.e., when communities are structurally well separated and thus intrinsically harder to hide. At  $\mu = 0.01$ , FCom-DICE yields the highest relative gain:  $M_1$  exceeding 2,000% change in  $\sigma_c \in [1.0, 2.0]$ , and  $M_2$  exceeding 500% in  $\sigma_c \in [0.5, 1.0, 2.0]$ . However, as  $\mu$  increases, the relative improvement diminishes but still shows at least an 8.2% difference over DICE in  $M_1$  and 2.1% in  $M_2$  when  $\sigma_c = 0.01$  (when node features are overlapping the most). Intuitively, when  $\sigma_c$  is very low and  $\mu$  is high, it becomes difficult to distinguish clusters in both the node feature space and the topological structure. Consequently, improvements over DICE are minimal, since the DICE method, which is considered state-of-the-art, already performs

well at hiding communities within a noisy network. Therefore, incorporating feature-aware edge attachment and modifying node features to align with the average of the attaching community does not significantly enhance hidability, as the node features lack sufficient separability already.

The effect of  $\sigma_c$ , however, is not linear, but both,  $\overline{\Delta M_1}(\mu, \sigma_c)$  and  $\overline{\Delta M_2}(\mu, \sigma_c)$ , peak at moderate  $\sigma_c$ . The largest relative gains tend to occur around  $\approx 0.5 - 2.0$ . A plausible explanation for this pattern might be provided by the GNN learning, particularly how DMoN learns clusters by optimizing modularity. Clusters are easily separable in node features  $\mathbf{X}$  when  $\sigma_c$  is large ( $\sigma_c = 5$ ). As a result, when  $\mu$  is low, the graph structure also reinforces this separation because the majority of edges stay within a community. FCom-DICE outperforms the baseline DICE, as random nodes selected inside the target community  $C^*$  are not only attached to other communities but also change their features to match the attached community. This simultaneously weakens  $C^*$  structurally and makes those nodes easier for DMoN to assign elsewhere.

However, when  $\mu$  is high (and  $\sigma_c$  is large),  $C^*$  already has many external edges relative to its internal edges. Structurally, this means communities are less separable and therefore make modularity-based clustering harder for DMoN even before any attack. At

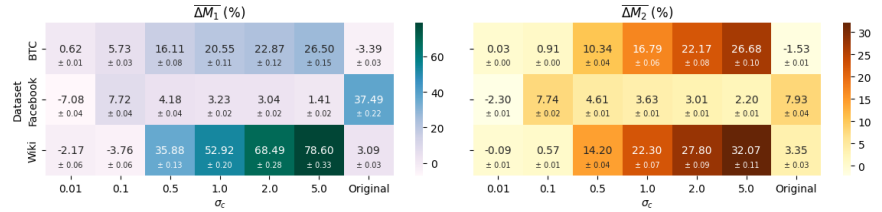


Figure 7: Average relative improvement (%) with  $\pm 1$  s.d. of FCom-DICE over baseline DICE averaged over all  $\beta_b$  and all realizations. The relative performance difference is illustrated for real networks with node features produced by a multivariate Gaussian distribution with varying  $\sigma_c$  (refer to Section 4.2 for methodological details) and original features (right column).

the same time, high  $\sigma_c$  makes communities highly distinct in the feature space. When DICE perturbs edges, leading to more noise in the structure, a GNN such as DMoN observes nodes from  $C^*$  densely connected to other communities, so during message passing, their features get pulled toward those neighboring communities. Because the neighboring communities have clean, well-defined feature signals, these boundary nodes of  $C^*$  acquire embeddings that resemble the external communities rather than  $C^*$ . As a result, when  $\mu$  is high, baseline DICE already hides  $C^*$  quite effectively, which leaves less room for FCom-DICE to improve over it.

Overall, FCom-DICE surpasses DICE, especially demonstrating significant relative improvement in networks with low  $\mu$ . It is important to note that the perturbations introduced by FCom-DICE do not alter the overall network community structure, as the community structure remains largely unchanged after the perturbation, even with significant perturbation budgets (refer to Appendix A.5). In addition, compared to DICE, FCom-DICE requires only a perturbation budget of 20-30% to reach the high plateau of hidability (see Appendix A.4 for details).

**Results on Real Networks.** We evaluated the performance of FCom-DICE against the baseline DICE on three real networks: Wikipedia, Facebook and Bitcoin Transactions. These datasets differ in size, sparsity, attribute dimensionality, and the semantics of their provided labels. Detailed dataset statistics, generated community labels, and node fea-

tures are described in Appendix A.6.

Figure 7 reports the relative improvement of  $\overline{\Delta M}_1(\text{Dataset}, \sigma_c)$  and  $\overline{\Delta M}_2(\text{Dataset}, \sigma_c)$ , across different values of  $\sigma_c$ , where  $\sigma_c$  controls the variance of node features generated from a multivariate Gaussian distribution (see Section 4.2 for detailed methodology).

Across all three datasets we observe that FCom-DICE consistently improves concealment compared to structure-only DICE as  $\sigma_c$  increases. The effect is most pronounced on Wikipedia, where higher  $\sigma_c$  features lead to large relative gains in both metrics. On Bitcoin Transactions, improvements are moderate, which could be reflecting the sparse and weakly modular nature of the network. Facebook exhibits the smallest overall improvement across all  $\sigma_c$  values (most improvement at  $\sigma_c = 0.1$ ). However, with original features, the results for the Facebook network are considerably higher for  $M_1$ . For low values of  $\sigma_c$ , corresponding to overlapping and noisy features, we observe little to no improvement, and in some cases small negative relative gain. This is aligned with findings on LFR, indicating that with noisy features, FCom-DICE offers limited additional leverage beyond structure-only attacks.

## 6 Related Work

Our research builds upon prior work in (i) community hiding for classical methods and (ii) community hiding for GNN-based clustering. While the GNN

literature on adversarial attacks is sizable, it primarily targets node classification [66, 62] or link prediction [61]; concealment from unsupervised GNN clustering remains underexplored, and most existing community-hiding approaches still rely on structural rewiring while largely ignoring feature-space perturbations.

**Community Hiding.** The robustness of community detection methods has been studied in the literature across three primary categories, distinguished by the scale of the manipulation: target node hiding [9], target community hiding [36], and global community structure attacks [60]. We focus on the mesoscale problem of *target community hiding*, i.e., dispersing a single community so it is not recovered as a coherent cluster. Early work in community hiding was proposed by Nagaraja in 2010 [36], who explored to what extent adding the small number of edges to the high-centrality nodes can provide privacy to a group of nodes defending from eavesdropping of the network traffic, i.e., avoid being detected in the cluster. The study showed that strategically placed cross-partition links reduce an eavesdropper’s ability to infer community structure, thereby enhancing privacy for the defended group. Subsequent papers formulated hiding as budgeted edge perturbation under deception objectives, including community safeness and related scores [13, 10], entropy-based fitness for genetic search [8], permanence-driven objectives [33], and escape/dispersion score [7]. A widely used baseline is DICE [58], a modularity-motivated heuristic that randomly deletes intra-community edges and adds cross-community edges without optimizing a specific score.

**Community Hiding from GNN.** Research work that explicitly targets community hiding from graph learning is sparse. One of the closely related works is an adversarial attack on graph-learning-based community detection known as CD-Attack [29]. The method trains a surrogate GNN community detector with a normalized-cut loss and perturbs edges (addition/deletion) around a target group of nodes via a constrained graph generator. A related ap-

proach, GCH [30], uses a graph autoencoder to select structural edits that suppress a community’s recoverability. Note that in both methods the perturbation is topology-only. Recent evaluations of GNN robustness for community detection reinforce that both edge and feature perturbations degrade clustering quality across different GNN architectures, but these works are diagnostic rather than prescriptive attacks [19]. This leaves a gap for methods that utilize structure and features to hide communities from GNN-based unsupervised clustering – a gap our work fills.

## 7 Discussion and Conclusion

This work illustrates how a targeted community can be concealed from GNN-based community detection by expanding DICE into FCom-DICE. Our work was inspired by literature documenting the importance of group privacy for personal safety and political freedom [4].

Our analysis shows that two factors majorly govern hidability: (i) the ratio of external to internal edges and (ii) the feature-space proximity of the target community to other communities. Guided by these findings, we proposed *FCom-DICE*, a feature-aware extension of DICE that deletes intra-community edges, adds cross-community edges toward the most feature-similar community, and applies feature modifications to match the linked community. Across featurized LFR graphs with ground truth evaluated with DMoN, FCom-DICE consistently outperforms structure-only baseline DICE and reaches strong concealment at smaller perturbation budgets. FCom-DICE also performs better than the baseline on featurized real networks, particularly when features are distinct to each community. However, FCom-DICE and DICE perform similarly when features overlap significantly or are excessively noisy.

**Implications.** From a privacy perspective, our findings suggest two complementary strategies for protecting high-value communities: limiting the formation of dense, internally isolated clusters (enhancing cross-community ties) and reducing feature distinctiveness relative to other communities. These re-

sults highlight how collective structure and attributes jointly contribute to group-level privacy leakage in graph learning pipelines.

Conversely, defenders aiming to identify concealed adversarial clusters or communities within the network should focus on structural and feature signals, such as abrupt increases in external/internal edge ratios for a community or feature drifts towards other communities. Further research is necessary to investigate techniques that can enhance the robustness of GNN methods against this issue.

**Limitations.** In our work we encourage researchers to consider a few limitations. First, perturbation budget  $b$  accounts for edge perturbations only; feature perturbations are considered as a part of that perturbation, as node features are changed based on the selection of the node in the edge addition. Thus, we assume it is a sub-process of that perturbation. In other studies that consider feature perturbation as an attack on GNN, features were manipulated independently from edge perturbations [66, 63]. Future work should model separate costs and plausibility constraints for feature perturbations. Secondly, node features are generated using a Gaussian distribution, which limits the generality of our findings. Future work should explore alternative featurization methods, including cases where node features do not align with ground-truth communities or that better mimic attribute distributions observed in real-world datasets. Third, our method FCom-DICE takes into account comprehensive network knowledge, including community structure and features, presuming that the defender aiming to obscure a high-value community possesses such information. Exploring scenarios involving partial or complete absence of such knowledge is a promising avenue.

## Acknowledgments

This paper has been coauthored by UT-Battelle, LLC under Contract No. DE-AC05-00OR22725 with the U.S. Department of Energy. The publisher, by accepting the article for publication, acknowledges that the U.S. government retains a nonexclusive, paid up, irrevocable, world-wide license to publish or re-

produce the published form of the manuscript, or allow others to do so, for U.S. government purposes. The DOE will provide public access to these results in accordance with the DOE Public Access Plan (<http://energy.gov/downloads/doe-public-access-plan>). This material is based upon work supported by the U.S. Department of Energy, Office of Science, Office of Advanced Scientific Computing Research under Contract No. DE-AC05-00OR22725. The funders had no role in study design, data collection and analysis, decision to publish, or preparation of this manuscript.

The work is also supported by the U.S. Department of Homeland Security award #17STQAC00001-07-00 and NSF Grant No. TI 2449402. Any opinions, findings, and conclusions or recommendations expressed in this material are those of the author(s) and do not necessarily reflect the views of the National Science Foundation nor the Department of Homeland Security.

Experiments were conducted using HPC resources provided by the Indiana University Pervasive Technology Institute (supported in part by the Lilly Endowment, Inc.).

## Ethical Considerations

This study strictly follows ethical guidelines and responsibilities, ensuring adherence to established standards for responsible security and AI research. In particular, we carefully consider the dual-use nature of techniques for analyzing and manipulating graph-learning systems and aim to maximize defensive value while minimizing potential harm.

### Identification of Stakeholders

**Researchers:** Those advancing the field by building upon this work, including researchers studying adversarial robustness, trustworthy GNNs, and defensive analysis of graph-based learning systems. This includes researchers developing countermeasures against adversarial groups seeking to hide coordinated activity from detection.

**Developers and Practitioners of AI Systems:** Individuals and organizations implementing or deploying GNN-based methods in real-world graph-related applications, including fraud detection in financial transaction networks, social networks, web traffic analysis, online auction networks, intrusion detection, software vulnerability detection, and monitoring of critical infrastructure systems.

**End-users:** Individuals whose activities, relationships, or assets are represented as nodes or edges in graph-based systems, including users of social networks, recommender systems, financial platforms, and digital services, as well as personnel, devices, or organizational units embedded within operational or infrastructure networks.

**Society at Large:** Broader communities and institutions impacted by the deployment of graph-based AI technologies, particularly in sensitive domains such as social networks, digital identity and fingerprinting, critical infrastructure, healthcare, and finance.

### Potential Risks for Stakeholders and Mitigations

#### For Researchers.

*Potential Risk:* The techniques presented and dis-

cussed in this work may be abused by adversaries to systematically evade GNN-based community or unsupervised clustering detection. Furthermore, the discussions of the methods presented in the paper lower the barrier for adversaries seeking methods of evasion and provide information that may lead to methods other than those discussed in this work. Additionally, the results of the suggested method’s concealment, which show that a target community can be effectively hidden under particular assumptions and perturbation budgets, run the risk of being misunderstood as offering more extensive guarantees than those found in the evaluated conditions.

*Mitigation:* By emphasizing defensive interpretation and refraining from assertions of universal applicability, we aim to minimize the risk of our findings being misappropriated or excessively generalized. The reported results are empirical and conditional on specific modeling assumptions, perturbation budgets, and graph properties. The proposed method and analysis of concealment are diagnostic approaches to investigate the robustness of GNN-based clustering systems and approaches of concealment, rather than turnkey evasion tools. We also emphasize that understanding the vulnerabilities of these systems is necessary for creating detection and auditing tools (e.g., for financial and computer network systems) and robust GNN architectures. We encourage the development of advanced detection and robustness techniques, especially in collaboration with ethics experts to ensure that the research aligns with best practices for responsible AI development.

#### For Developers and Practitioners.

*Potential Risk:* The proposed defense-oriented insights and methods may not generalize to all graph-learning architectures, datasets, or deployment contexts, potentially leading to misplaced confidence.

*Mitigation:* We encourage comprehensive empirical validation across diverse GNN architectures, datasets, and threat assumptions prior to deployment.

#### For End-users.

*Potential Risk:* The findings in this work indicate that coordinated groups may intentionally alter structural and feature signals to evade GNN-based community detection. As a result, end-users may

be indirectly exposed to greater harm if malicious or harmful clusters (e.g., fraudulent transactions, scam activity or coordinated abuse behavior) remain undetected for longer periods. Furthermore, the implementation of the proposed concealment method to obscure a group may adversely affect its members, as altered features and connections could result in learned embeddings that misrepresent the individuals within the system.

*Mitigation:* To reduce potential harm to end-users, GNN-based cluster detection systems should not be deployed as the sole mechanism for identifying malicious or coordinated activity. And when concealment methods or feature-aware perturbations are used, practitioners should limit the downstream use of learned embeddings, particularly for individual-level decisions and recommendations.

#### For Society.

*Potential Risk:* Community hiding techniques discussed in this paper may support privacy and freedom of association by helping benign groups resist intrusive surveillance, aggressive profiling, or targeted advertising based on social graph inference. [4] Additionally, understanding how attackers identify targets can help critical infrastructure operators protect high-value clusters and sensitive dependencies from adversarial reconnaissance. However, if widely available, such techniques could enable coordinated malicious actors (e.g., fraud networks, social influence operations or organized cybercrime groups) to evade detection and persist longer, increasing financial, social, or safety-related harm. At scale, these dynamics may incentivize more expansive or indiscriminate monitoring, raising the risk of over-surveillance and collateral harm to benign communities, thereby exacerbating social inequities, privacy breaches, or manipulation of vulnerable populations.

*Mitigation:* Balancing AI security advancements with societal considerations (including fairness, transparency, and accountability) mitigates potential harm. Ethical implications for vulnerable populations should be addressed, prioritizing societal well-being.

## Considerations Motivating Ethical-Related Decisions

**Research Goal:** The primary objective of this work is to improve understanding of how GNN-based community detection can be evaded and to inform the design of more robust and trustworthy systems. The proposed method illustrates how communities can be obscured, serving as a defensive strategy against adversarial threats or as a means of safeguarding the privacy of vulnerable groups.

## Benefits and Harms

**Benefits:** Enhanced techniques for obscuring and thereby safeguarding high-value clusters and at-risk communities from adversarial GNN-based detection systems; improved understanding of the robustness of GNN-based unsupervised clustering.

**Harms:** Potential empowerment of malicious actors and overestimating the effectiveness of the proposed defense method.

**Rights:** This work implicates rights related to privacy, freedom of association, and fair representation in algorithmic systems. As graph-based learning models infer relationships and group membership from potentially sensitive structural and feature information, our findings underscore the importance of guarding against unjustified profiling, misrepresentation, or automated decisions based solely on inferred graph structure.

## Awareness of Ethical Perspectives

We acknowledge different ethical perspectives on the disclosure of community hiding techniques. While transparency is essential for identifying vulnerabilities and strengthening defenses, particularly for protecting privacy and critical infrastructure, such techniques may also be misused to evade detection. It is also essential for revealing evasion techniques and motivating improvements in GNN-based community detection. This work frames community hiding as a dual-use capability and focuses on defensive analysis under explicit assumptions, with the goal of supporting responsible interpretation and strengthening

future graph-learning methods.

## A Appendix

### A.1 Details on DICE Performance

Figure 8 illustrates the isolated impact of structural noise, depicting the average rate of change relative to budget as a function of  $\mu$ , averaged across all  $\sigma_c$ . As  $\mu$  increases, the average rate of change in  $M_1$  also increases, while the average rate of change in  $M_2$  rises to a maximum at  $\mu = 0.3$  before experiencing a slight decline thereafter.

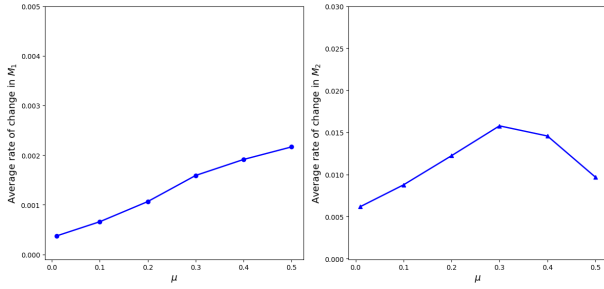


Figure 8: Average rate of change of  $M_1$  and  $M_2$  vs.  $\mu$ , averaged over  $\sigma_c$ .

### A.2 Interpretable ML

Our goal in this work is to identify the characteristics of communities that affect their hidability. We use interpretable ML, particularly feature importance analysis [34], to find these characteristics.

In *feature importance* methods, input variables of a model (e.g., regression) are scored to assess their contribution to the prediction output. Popular methods such as mean decrease impurity (MDI) [31] and permutation importance [6], can be biased toward high-cardinality features [51] or yield misleading results when features are highly correlated [40]. SHAP (SHapley Additive exPlanations) [32], on the other hand, addresses some of these issues and provides a theoretically grounded explanation of model prediction based on Lloyd Shapley’s approach to cooperative games [46]. The method outlines that the

contribution  $\phi_i$  of each feature  $i$  is computed as its average marginal effect across all possible subsets of other features. The prediction for the input variable  $x$  is then the additive sum of all  $M$  features’ contributions,  $f(x) = \phi_0 + \sum_{i=1}^M \phi_i$ , where  $\phi_0$  is the expected value of the model prediction, and  $\phi_i$  is the contribution of the  $i$ -th feature.

Unlike heuristic importance measures, SHAP ensures each feature’s contribution is additive and consistent. When a feature has a stronger effect in a modified model, its attribution cannot decrease. For correlated features, credit distribution should be fair and not favor one feature over another [32].

In this study, we leverage SHAP to identify which network-level and statistical descriptors most strongly influence the detectability of hidden communities. Note that our framework allows the usage of other interpretable techniques (e.g., LIME [44]), but due to robustness and consistency, we report only results based on SHAP [67, 45].

### A.3 Details on SHAP Analysis

Figure 9 illustrates the summary of the SHAP analysis (beeswarm plot), which offers a comprehensive overview of SHAP values ( $M_1$  in Figure 9a,  $M_2$  in Figure 9b) for the feature set (refer to Table 2) arranged by their impact. Note that linear regression was rejected due to violated model assumptions and instead, Random Forest Regression was used to capture nonlinear relationships without distributional constraints.

### A.4 Comparison of FCom-DICE with DICE

The proposed method, *FCom-DICE*, yields a noticeable performance improvement over DICE (baseline). In Figure 10a, both  $M_1$  (top row) and  $M_2$  (bottom row) still increase with the perturbation budget  $\beta_b$ , and at the same time the overall trend of growing hidability with higher  $\mu$  and lower  $\sigma_c$  still holds. However, with *FCom-DICE*, performance increases faster, particularly for larger  $\mu$  (e.g.,  $\mu = 0.3$  or  $0.5$ ), reaching a plateau value at a lower (around 20-30%) perturbation budget  $\beta_b$ , rather than increasing gradually

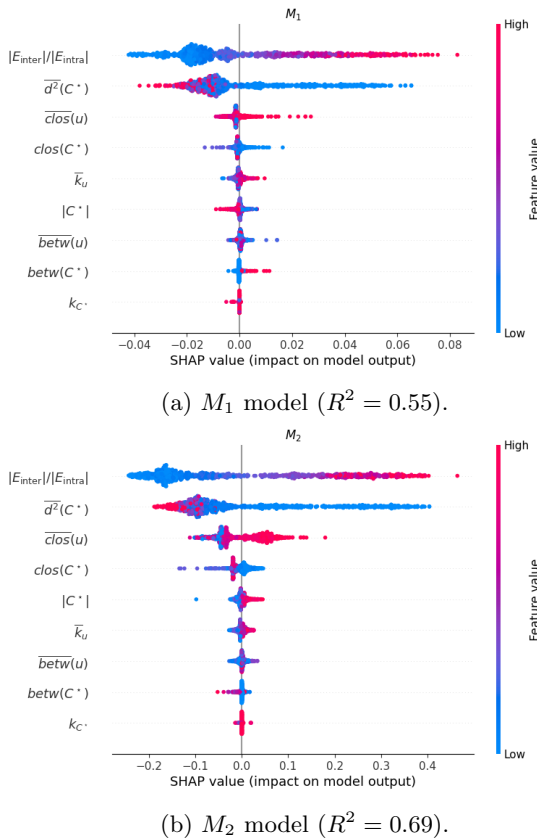


Figure 9: SHAP summary plots for Random Forest Regression of community hidability.

across the full budget range, as observed for DICE (Fig. 10b). For instance, at  $\mu = 0.5$  a low  $\sigma_c$ ,  $M_2$  rises to  $\approx 0.8$  after less than 20% of the budget, suggesting that the cap of the hiding capacity is achieved with a smaller perturbation compared to DICE.

### A.5 Structural Similarity after FCom-DICE

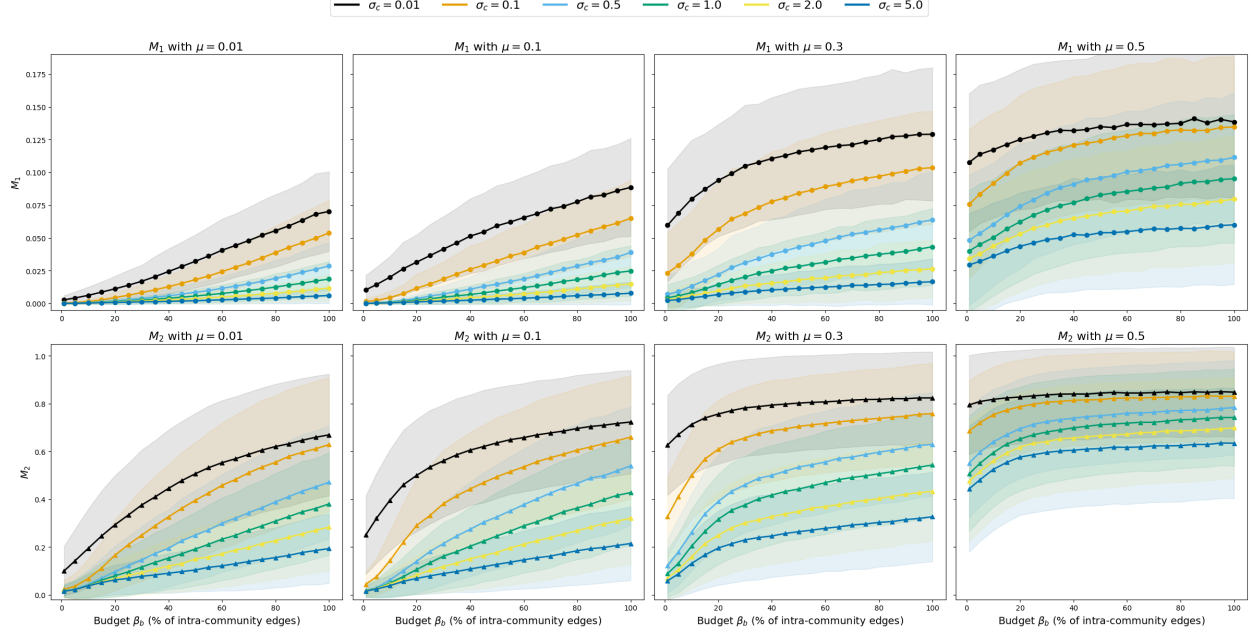
We quantify global community structure similarity between the original and perturbed graphs using the Element-Centric Similarity (ECS) [17], which has been used before to compare the community structures before and after the network perturbation and test the robustness of the community structure [60, 19].

Figure 11 shows that ECS remains largely stable across the full range of perturbation budgets  $\beta_b$  for all tested  $\mu$  and  $\sigma_c$  values. Although the absolute ECS level shifts with different  $\mu$  and  $\sigma_c$ , the curves are nearly flat with respect to  $\beta_b$ , indicating that increasing the budget does not create structural distortion in the graph. This suggests that even at high perturbation levels the overall network community structure, as captured by ECS, remains largely preserved.

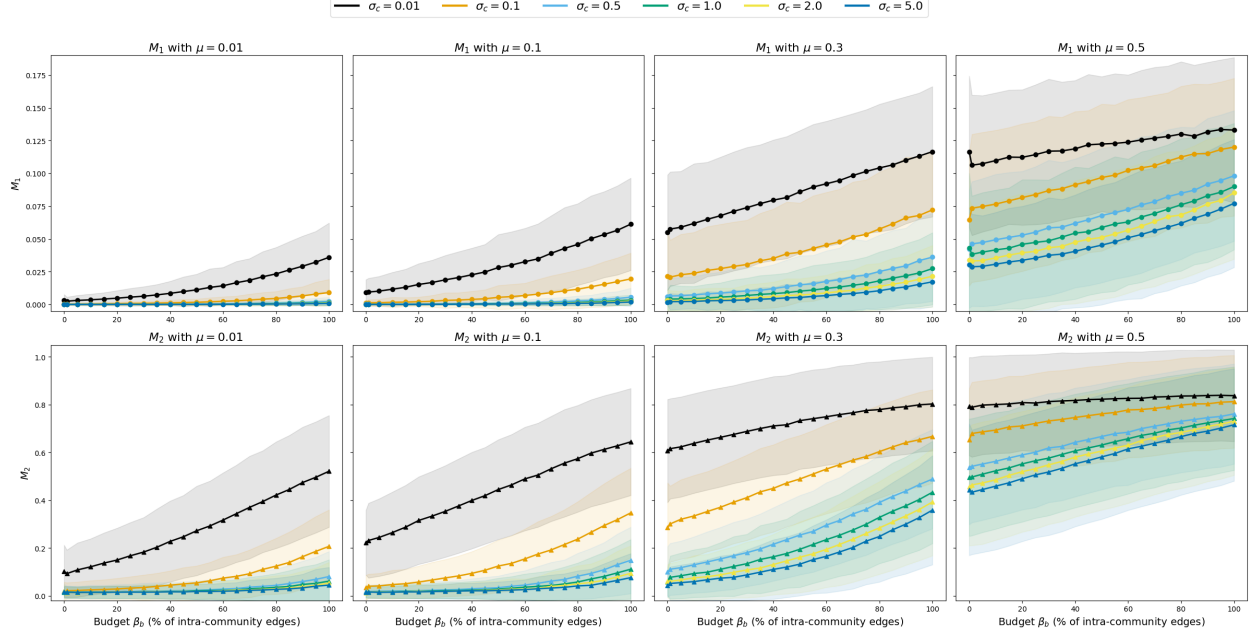
### A.6 Experimental Details on Real Networks

We use real attributed networks provided by PyTorch Geometric. For Wikipedia and Facebook, we used **AttributedGraphDataset** class [64]. For Bitcoin Transactions (BTC), we used the Elliptic Bitcoin dataset [59] and limited analysis to the largest connected component to sample a sizable network of transactions.

**Community Labels.** The node labels provided with the real-world datasets considered in this study are not intended to represent ground-truth communities. Instead, they encode dataset-specific metadata whose semantics might not reflect a community or cluster in a graph. For Facebook, the graph is constructed from ego networks of users (nodes), and the provided labels correspond to ego-centric user attributes. These labels, which contain a lot of singleton classes, are therefore considered unsuitable for



(a) *FCom-DICE*.



(b) *DICE* (baseline).

Figure 10: Comparison of *FCom-DICE* and *DICE* performance across  $\sigma_c$ ,  $\mu$ , and perturbation budget  $\beta_b$  ( $p = 0.5$ ). Shaded bands denote  $\pm 1$  s.d. across runs.

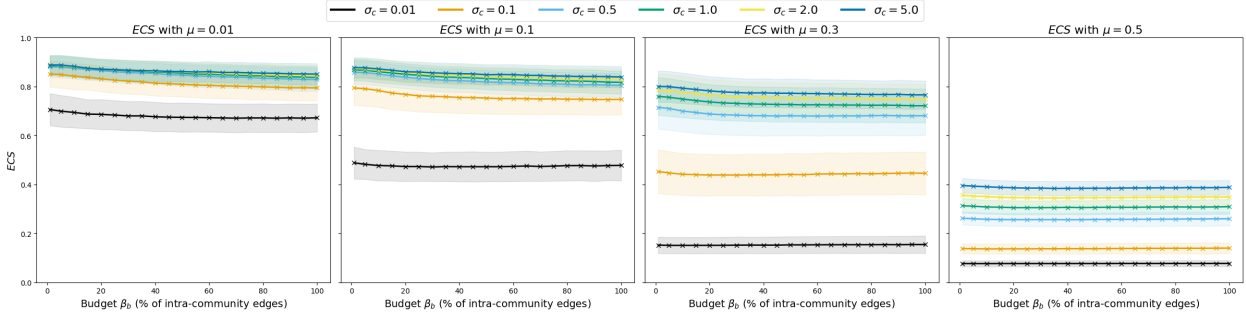


Figure 11: ECS of *FCom-DICE* across  $\sigma_c$ ,  $\mu$ , and perturbation budget  $\beta_b$  ( $p = 0.5$ ). Shaded bands denote  $\pm 1$  s.d. across runs.

Table 4: Statistics of real-world datasets used in evaluation.

	Wiki	Facebook	BTC*
Nodes	2,405	4,039	7,880
Edges	11,596	88,234	9,164
Density	0.0040	0.0108	0.0003
Modularity	0.505	0.482	0.217
Original Features	4,973	1,283	165
Provided Labels	17	151	3
$ \mathcal{C}_{\text{consensus}} $	58	16	39

Note:  $|\mathcal{C}_{\text{consensus}}|$  denotes the number of community labels obtained via consensus Louvain.

\* The largest connected component (LCC) of the Bitcoin Transactions network was used.

the community hiding downstream tasks covered in the paper. In Wikipedia’s page-to-page hyperlink network, node labels correspond to topical categories assigned to pages (nodes). While semantically meaningful, these categories are broad and not defined by network connectivity and frequently span multiple structural communities. For Bitcoin Transactions, only three labels are provided, indicating whether a transaction is classified as licit, illicit, or unknown. These classes reflect transactional status rather than structural organization and therefore cannot be interpreted as communities. Therefore, we do not treat the provided labels as ground-truth communities and do not evaluate methods against the provided labels. Moreover, apart from the arguments described, prior

work has repeatedly shown that metadata labels in real networks often exhibit weak or inconsistent alignment with communities detected [21, 43].

Instead of relying on dataset-provided labels, we derive structural community assignments using consensus clustering based on the Louvain algorithm [3], which is a widely used modularity-maximization method that is considered well suited for large real-world networks. As Louvain is stochastic and may produce different partitions across runs, we obtain a stable community label using the consensus clustering method [27]. Consensus clustering identifies pairs of nodes that consistently co-occur in the same community across repeated Louvain runs, constructs an agreement matrix encoding co-assignment frequencies, and retains only node pairs whose co-assignment frequency exceeds a threshold  $\tau$ , reclustering this agreement to produce the final consensus partition.

In our experiments, we compute Louvain consensus clustering using 50 independent runs and set  $\tau = 0.3$ , consistent with reported high accuracy [27]. Note that consensus Louvain is used only to define a stable reference partition.

## References

- [1] Arif Ali, Abdur Rasheed, Afaq Siddiqui, Maliha Naseer, Saba Wasim, and Waseem Akhtar. Non-parametric test for ordered medians: The jonckheere terpstra test. *International Journal of*

*Statistics in Medical Research*, 4:203–207, May 2015.

[2] Riju Bhattacharya, Naresh Kumar Nagwani, and Sarsij Tripathi. A community detection model using node embedding approach and graph convolutional network with clustering technique. *Decision Analytics Journal*, 9:100362, December 2023.

[3] Vincent D Blondel, Jean-Loup Guillaume, Renaud Lambiotte, and Etienne Lefebvre. Fast unfolding of communities in large networks. *Journal of Statistical Mechanics: Theory and Experiment*, 2008(10):P10008, March 2008.

[4] Joseph Bonneau, Jonathan Anderson, Ross Anderson, and Frank Stajano. Eight friends are enough: social graph approximation via public listings. In *Proceedings of the Second ACM EuroSys Workshop on Social Network Systems*, SNS '09, pages 13–18, New York, NY, USA, March 2009. Association for Computing Machinery.

[5] U. Brandes, D. Delling, M. Gaertler, R. Goerke, M. Hoefer, Z. Nikoloski, and D. Wagner. Maximizing Modularity is hard, August 2006. arXiv:physics/0608255.

[6] Leo Breiman. Random Forests. *Machine Learning*, 45(1):5–32, October 2001.

[7] Zhengchao Chang, Jing Liang, Shaohui Ma, and Dong Liu. Community hiding: Completely escape from community detection. *Information Sciences*, 672:120665, June 2024.

[8] Jinyin Chen, Yixian Chen, Lihong Chen, Minghao Zhao, and Qi Xuan. Multiscale Evolutionary Perturbation Attack on Community Detection. *IEEE Transactions on Computational Social Systems*, 8(1):62–75, February 2021.

[9] Jinyin Chen, Yangyang Wu, Xuanheng Xu, Yixian Chen, Haibin Zheng, and Qi Xuan. Fast Gradient Attack on Network Embedding. *ArXiv*, September 2018.

[10] Xianyu Chen, Zhongyuan Jiang, Hui Li, Jianfeng Ma, and Philip S. Yu. Community Hiding by Link Perturbation in Social Networks. *IEEE Transactions on Computational Social Systems*, 8(3):704–715, June 2021.

[11] Aaron Clauset, M E J Newman, and Christopher Moore. Finding community structure in very large networks. *Phys. Rev. E Stat. Nonlin. Soft Matter Phys.*, 70(6 Pt 2):066111, December 2004.

[12] Valeria Fionda and Giuseppe Pirrò. From Community Detection to Community Deception, September 2016. arXiv:1609.00149 [cs].

[13] Valeria Fionda and Giuseppe Pirrò. Community Deception or: How to Stop Fearing Community Detection Algorithms. *IEEE Transactions on Knowledge and Data Engineering*, 30(4):660–673, April 2018.

[14] Santo Fortunato. Community detection in graphs. *Physics Reports*, 486(3):75–174, 2010.

[15] Linton C. Freeman. A Set of Measures of Centrality Based on Betweenness. *Sociometry*, 40(1):35–41, 1977.

[16] Linton C. Freeman. Centrality in social networks conceptual clarification. *Social Networks*, 1(3):215–239, January 1978.

[17] Alexander J. Gates, Ian B. Wood, William P. Hetrick, and Yong-Yeol Ahn. Element-centric clustering comparison unifies overlaps and hierarchy. *Scientific Reports*, 9(1):8574, June 2019.

[18] M. Girvan and M. E. J. Newman. Community structure in social and biological networks. *Proceedings of the National Academy of Sciences*, 99(12):7821–7826, June 2002.

[19] Jaidev Goel, Pablo Moriano, Ramakrishnan Kannan, and Yulia R. Gel. Community detection robustness of graph neural networks, September 2025. arXiv:2509.24662 [cs].

[20] William L. Hamilton, Rex Ying, and Jure Leskovec. Inductive representation learning on large graphs. In *Proceedings of the 31st International Conference on Neural Information Processing Systems*, NIPS’17, pages 1025–1035, Red Hook, NY, USA, December 2017. Curran Associates Inc.

[21] Darko Hric, Richard K. Darst, and Santo Fortunato. Community detection in networks: Structural communities versus ground truth. *Physical Review E*, 90(6):1–19, 2014.

[22] A. R. Jonckheere. A Distribution-free k-sample test against ordered alternatives. *Biometrika*, 41(1-2):133–145, June 1954. tex.eprint: <https://academic.oup.com/biomet/article-pdf/41/1-2/133/1244074/41-1-2-133.pdf>.

[23] Thomas Kipf and M. Welling. Variational Graph Auto-Encoders. In *NeurIPS Workshop on Bayesian Deep Learning (NeurIPS BDL)*, November 2016.

[24] Thomas N. Kipf and Max Welling. Semi-Supervised Classification with Graph Convolutional Networks. In *International Conference on Learning Representations*, February 2017.

[25] Günter Klambauer, Thomas Unterthiner, Andreas Mayr, and Sepp Hochreiter. Self-Normalizing Neural Networks. In *Advances in Neural Information Processing Systems*, volume 30. Curran Associates, Inc., 2017.

[26] Andrea Lancichinetti. Community detection algorithms: A comparative analysis. *Physical Review E*, 80(5), 2009.

[27] Andrea Lancichinetti and Santo Fortunato. Consensus clustering in complex networks. *Scientific Reports*, 2(1):336, March 2012.

[28] Andrea Lancichinetti, Santo Fortunato, and Filippo Radicchi. Benchmark graphs for testing community detection algorithms. *Physical Review E*, 78(4):046110, October 2008.

[29] Jia Li, Honglei Zhang, Zhichao Han, Yu Rong, Hong Cheng, and Junzhou Huang. Adversarial Attack on Community Detection by Hiding Individuals. In *Proceedings of The Web Conference 2020*, pages 917–927, April 2020.

[30] Dong Liu, Zhengchao Chang, Guoliang Yang, and Enhong Chen. Community hiding using a graph autoencoder. *Knowledge-Based Systems*, 253:109495, October 2022.

[31] Gilles Louppe. *Understanding Random Forests: From Theory to Practice*. PhD thesis, University of Liege, Belgium, 2014.

[32] Scott M. Lundberg and Su-In Lee. A unified approach to interpreting model predictions. In *Proceedings of the 31st International Conference on Neural Information Processing Systems*, NIPS’17, pages 4768–4777, Red Hook, NY, USA, December 2017. Curran Associates Inc.

[33] Shravika Mittal, Debarka Sengupta, and Tanmoy Chakraborty. Hide and Seek: Outwitting Community Detection Algorithms. *IEEE Transactions on Computational Social Systems*, 8(4):799–808, August 2021.

[34] Christoph Molnar. *Interpretable Machine Learning*. Lulu.com, 2020. Google-Books-ID: jBm3DwAAQBAJ.

[35] Pablo Moriano, Jorge Finke, and Yong-Yeol Ahn. Community-Based Event Detection in Temporal Networks. *Scientific Reports*, 9(1):4358, March 2019.

[36] Shishir Nagaraja. The Impact of Unlinkability on Adversarial Community Detection: Effects and Countermeasures. In Mikhail J. Atallah and Nicholas J. Hopper, editors, *Privacy Enhancing Technologies*, pages 253–272, Berlin, Heidelberg, 2010. Springer.

[37] M E J Newman. Finding community structure in networks using the eigenvectors of matrices. *Phys. Rev. E*, 74(3):036104, September 2006.

[38] M. E. J. Newman. Modularity and community structure in networks. *Proceedings of the National Academy of Sciences of the United States of America*, 103(23):8577–8582, June 2006.

[39] M. E. J. Newman and M. Girvan. Finding and evaluating community structure in networks. *Phys. Rev. E*, 69(2):026113, February 2004.

[40] Kristin K. Nicodemus, James D. Malley, Carolin Strobl, and Andreas Ziegler. The behaviour of random forest permutation-based variable importance measures under predictor correlation. *BMC Bioinformatics*, 11(1):110, February 2010.

[41] Diogo Pacheco, Pik-Mai Hui, Christopher Torres-Lugo, Bao Tran Truong, Alessandro Flammini, and Filippo Menczer. Uncovering Coordinated Networks on Social Media: Methods and Case Studies. *Proceedings of the International AAAI Conference on Web and Social Media*, 15:455–466, May 2021.

[42] Chanyoung Park, Donghyun Kim, Jiawei Han, and Hwanjo Yu. Unsupervised Attributed Multiplex Network Embedding. *Proceedings of the AAAI Conference on Artificial Intelligence*, 34(04):5371–5378, April 2020.

[43] Leto Peel, Daniel B. Larremore, and Aaron Clauset. The ground truth about metadata and community detection in networks. *Science Advances*, 3(5):e1602548, May 2017.

[44] Marco Tulio Ribeiro, Sameer Singh, and Carlos Guestrin. "Why Should I Trust You?": Explaining the Predictions of Any Classifier. In *Proceedings of the 22nd ACM SIGKDD International Conference on Knowledge Discovery and Data Mining*, KDD '16, pages 1135–1144, New York, NY, USA, August 2016. Association for Computing Machinery.

[45] Wojciech Samek and Klaus-Robert Müller. Towards Explainable Artificial Intelligence. In Wojciech Samek, Grégoire Montavon, Andrea Vedaldi, Lars Kai Hansen, and Klaus-Robert Müller, editors, *Explainable AI: Interpreting, Explaining and Visualizing Deep Learning*, pages 5–22. Springer International Publishing, Cham, 2019.

[46] L. S. Shapley. 17. A Value for n-Person Games. In Harold William Kuhn and Albert William Tucker, editors, *Contributions to the Theory of Games (AM-28), Volume II*, pages 307–318. Princeton University Press, December 1953.

[47] Tom A. B. Snijders and Krzysztof Nowicki. Estimation and Prediction for Stochastic Blockmodels for Graphs with Latent Block Structure. *Journal of Classification*, 14(1):75–100, January 1997.

[48] Nitish Srivastava, Geoffrey Hinton, Alex Krizhevsky, Ilya Sutskever, and Ruslan Salakhutdinov. Dropout: A Simple Way to Prevent Neural Networks from Overfitting. *Journal of Machine Learning Research*, 15(56):1929–1958, 2014.

[49] Natalie Stanley, Roland Kwitt, Marc Niethammer, and Peter J. Mucha. Compressing Networks with Super Nodes. *Scientific Reports*, 8:10892, July 2018.

[50] Samuel A. Stouffer, Edward A. Suchman, Leland C. DeVinney, Shirley A. Star, and Robin M. Jr. Williams. *The American Soldier, Vol. 1: Adjustment during Army Life*. Princeton University Press, Princeton, NJ, 1949.

[51] Carolin Strobl, Anne-Laure Boulesteix, Achim Zeileis, and Torsten Hothorn. Bias in random forest variable importance measures: Illustrations, sources and a solution. *BMC Bioinformatics*, 8(1):25, January 2007.

[52] Leyla Tekin and Belgin Ergenç Bostanoğlu. A Qualitative Survey on Community Detection Attack Algorithms. *Symmetry*, 16(10):1272, October 2024. Number: 10.

[53] T.J. Terpstra. The asymptotic normality and consistency of kendall's test against trend, when ties are present in one ranking. *Indagationes Mathematicae (Proceedings)*, 55:327–333, 1952.

[54] V A Traag, L Waltman, and N J van Eck. From Louvain to Leiden: guaranteeing well-connected communities. *Sci. Rep.*, 9(1), December 2019.

[55] Anton Tsitsulin, John Palowitch, Bryan Perozzi, and Emmanuel Müller. Graph Clustering with Graph Neural Networks. *Journal of Machine Learning Research*, 24:1–21, June 2023.

[56] Anton Tsitsulin, Benedek Rozemberczki, John Palowitch, and Bryan Perozzi. Synthetic Graph Generation to Benchmark Graph Learning. In *NeurIPS 2022 GLFrontiers Workshop*, April 2022.

[57] Petar Veličković, Guillem Cucurull, Arantxa Casanova, Adriana Romero, Pietro Liò, and Yoshua Bengio. Graph Attention Networks. February 2018.

[58] Marcin Waniek, Tomasz P. Michalak, Michael J. Wooldridge, and Talal Rahwan. Hiding individuals and communities in a social network. *Nature Human Behaviour*, 2(2):139–147, February 2018.

[59] Mark Weber, Giacomo Domeniconi, Jie Chen, Daniel Karl I. Weidele, Claudio Bellei, Tom Robinson, and Charles E. Leiserson. Anti-Money Laundering in Bitcoin: Experimenting with Graph Convolutional Networks for Financial Forensics. In *KDD ’19 Workshop on Anomaly Detection in Finance*, July 2019.

[60] Zhi-Feng Wei, Pablo Moriano, and Ramakrishnan Kannan. Robustness of graph embedding methods for community detection, November 2024. arXiv:2405.00636 [physics].

[61] Fan Wu, Yunhui Long, Ce Zhang, and Bo Li. LINKTELLER: Recovering Private Edges from Graph Neural Networks via Influence Analysis. pages 2005–2024. IEEE Computer Society, May 2022.

[62] Zhaohan Xi, Ren Pang, Shouling Ji, and Ting Wang. Graph Backdoor. pages 1523–1540, 2021.

[63] Ying Xu, Michael Lanier, Anindya Sarkar, and Yevgeniy Vorobeychik. Attacks on Node Attributes in Graph Neural Networks, March 2024. arXiv:2402.12426 [cs].

[64] Renchi Yang, Jieming Shi, Xiaokui Xiao, Yin Yang, Sourav S. Bhowmick, and Juncheng Liu. PANE: scalable and effective attributed network embedding. *The VLDB Journal*, 32(6):1237–1262, November 2023.

[65] Zhao Yang, René Algesheimer, and Claudio J. Tessone. A Comparative Analysis of Community Detection Algorithms on Artificial Networks. *Scientific Reports*, 6(1):30750, August 2016.

[66] Daniel Zügner, Amir Akbarnejad, and Stephan Günnemann. Adversarial Attacks on Neural Networks for Graph Data. In *Proceedings of the 24th ACM SIGKDD International Conference on Knowledge Discovery & Data Mining*, KDD ’18, pages 2847–2856, New York, NY, USA, July 2018. Association for Computing Machinery.

[67] Erik Štrumbelj and Igor Kononenko. Explaining prediction models and individual predictions with feature contributions. *Knowledge and Information Systems*, 41(3):647–665, December 2014.